TRIBHUVAN UNIVERSITY

INSTITUTE OF ENGINEERING

PULCHOWK CAMPUS

THESIS NO: 078/MSPSE/006

Analysis of Effects of Loading Conditions on Condition Monitoring of Induction Machines

by

Chandan Pokhrel

A THESIS

SUBMITTED TO THE DEPARTMENT OF ELECTRICAL ENGINEERING IN PARTIAL FULFILLMENT OF THE REQUIREMENTS FOR THE DEGREE OF MASTER OF SCIENCE IN POWER SYSTEM ENGINEERING

DEPARTMENT OF ELECTRICAL ENGINEERING

LALITPUR, NEPAL

JULY, 2024

COPYRIGHT©

त्रिभुवन विश्वविद्यालय
TRIBHUVAN UNIVERSITY
इन्जिनियरिङ्ग अध्ययन संस्थान
INSTITUTE OF ENGINEERING
पुल्चोक क्याम्पस
PULCHOWK CAMPUS
DEPARTMENT OF ELECTRICAL ENGINEERING
Pulchowk, Lalitpur

Accredited by University Grants Commission (UGC) Nepal 2020

CERTIFICATE OF APPROVAL

The undersigned certify that they have read and recommended to the Institute of Engineering for acceptance, a dissertation entitled "**Analysis of Effects of Loading Conditions on Condition Monitoring of Induction Machines**", submitted by **Chandan Pokhrel** in partial fulfillment of the requirement for the award of the degree of **Master of Science in Power System Engineering**.

Prof. Dr. Nava Raj Karki
Supervisor
M.Sc. in Power System Engineering

Assoc. Prof. Dr. Basanta K. Gautam
Supervisor
M.Sc. in Power System Engineering

Prof. Dr. Rajesh Karki
External Examiner
University of Saskatchewan, Canada

Assoc. Prof. Dr. Basanta K. Gautam
Program Coordinator
M.Sc. in Power System Engineering

Asst. Prof. Yuba Raj Adhikari
Head of Department
Department of Electrical Engineering

June, 2024

Tel: +977-1-5443081, Email: doee@pcampus.edu.np, Website: www.doee.pcampus.edu.np

ABSTRACT

Induction machines are extensively utilized in various industries due to their cost effectiveness, robustness, and high efficiency. However, as with all electrical machines, they are prone to degradation over time, necessitating expensive repairs and maintenance. Detecting faults early is critical to minimizing unplanned downtime and reducing operational costs. One significant fault that can significantly impact the performance of induction machines is broken rotor bars.

Broken rotor bars can lead to various undesirable effects, including increased vibration, reduced efficiency, and potential catastrophic failure if left undetected. Motor current signature analysis (MCSA) is a widely adopted technique for monitoring the condition of induction machines during normal operation. By analyzing the frequency spectrum of the stator current, MCSA provides valuable insights into the health of the machine and can detect anomalies indicative of broken rotor bars.

This study specifically focuses on analyzing the stator current signals of a squirrel cage induction machine to detect and diagnose broken rotor bar faults under different load conditions. The research employs a multi-layer perceptron (MLP) model, a type of artificial neural network known for its ability to learn complex patterns, to study the impact of varying operational loads on fault detection accuracy.

To conduct the study, a dataset is divided into two parts: 75% for training the MLP models and 25% for testing and validation purposes. The performance of the MLP models is evaluated using a confusion matrix, which provides metrics such as accuracy, precision, recall, and F1-score across different load levels. These metrics offer a comprehensive assessment of the model's effectiveness in detecting broken rotor bar faults under realistic operating conditions.

By integrating MCSA with advanced machine learning techniques like MLPs, this research aims to enhance the reliability and efficiency of condition monitoring systems for induction machines. The findings contribute to the development of predictive maintenance strategies that can preemptively address faults like broken rotor bars, thereby optimizing machine uptime and minimizing maintenance costs.

Keywords: Induction Motor, Condition Monitoring, Fourier Transform, Broken Rotor Bars

ACKNOWLEDGEMENT

I would like to express my deepest gratitude to my supervisors, Prof. Dr. Nava Raj Karki and Associate Prof. Dr. Basanta Kumar Gautam, for their invaluable guidance, insightful comments, and continuous support and encouragement throughout the progress of this research work. Furthermore, I am immensely thankful to the whole team of Department of Electrical Engineering, IoE, Pulchowk Campus for providing the necessary resources and environment conducive to academic growth and learning.

I am also grateful for the opportunity to participate in student mobility under the Capacity Enhancement in Electrical Equipment Condition Monitoring and Fault Diagnosis (CEEECoM) project, co-funded by Erasmus+ program of the European Union. This experience not only enriched my academic journey but also broadened my perspectives, allowing me to engage with diverse cultures and academic traditions. The financial support provided under this project made it possible for me to pursue this invaluable learning experience abroad.

I express my sincere thanks go to Department of Electrical Engineering and Automation, Aalto University, Finland and to Prof. Anouar Belahcen and Nada El Bouharrouti for their precious suggestion and kind support throughout this research work.

Lastly, I would like to extend my appreciation to my friends and family for their unwavering encouragement and understanding during this challenging yet rewarding endeavor. Their moral support has been a constant source of strength throughout my academic pursuits.

This thesis would not have been possible without the contributions and support of all those mentioned above. Thank you all for believing in me and for being part of this journey.

TABLE OF CONTENTS

LIST OF FIGURES

LIST OF TABLES

LIST OF ABBREVIATIONS

BRB	Broken Rotor Bar
FFT	Fast Fourier Transform
FN	False Negative
FP	False Positive
LSB	Left Side Band
MCSA	Motor Current Signature Analysis
MLP	Multi Layer Perceptron
RSB	Right Side Band
TP	True Positive
TN	True Negative

CHAPTER ONE: INTRODUCTION

1.1 Background

An electric machine is a versatile electromechanical device capable of functioning as both a generator and a motor. When operated as a motor, it converts electrical energy into mechanical energy, playing a pivotal role in consuming more than 60% of the total global electrical power produced[1]. Electric motors are indispensable across industries, powering everything from industrial machinery and transportation systems to household appliances and automation equipment. Conversely, when serving as a generator, the electric machine transforms mechanical energy into electrical energy. This function is critical in generating the vast majority of the global electrical energy consumed across residential, commercial, and industrial sectors. Generators are essential for producing electricity in power plants, renewable energy installations, backup power systems, and various other applications where reliable electrical supply is must.

In the present world, electrical machines are extensively employed in diverse applications such as power generation, manufacturing industries, electric vehicles, and household appliances. These machines vary significantly in size, from small units of a few kilowatts for household use to large-scale units exceeding hundreds of megawatts for electricity generation. Whether operating independently or as integral components within complex systems, these machines must function seamlessly to ensure optimal performance. Hence, there is a critical need for these machines to operate reliably and consistently in order to fulfill their intended roles effectively.

There are various faults that could compromise the operation of the electrical machines. Many of these problems begin as slight deviations from normal operating conditions, and if not addressed promptly in their early stages, could lead to severe and potentially catastrophic failures.[2]. The continuous assessment of the operating conditions of the electrical machine and the plant for the early detection of faults and the targeted planning of the maintenance to avoid catastrophic failures is the condition monitoring. The advance warning of the faults allows us to schedule the maintenance in the most convenient manner. This helps to reduce the mean down time and increases the mean time between failures to ensure the high availability of the machines.

Condition monitoring involves continuously evaluating how well the machines and their individual components are performing. By collecting and analyzing real-time data on

their performance, any potential problems can be detected early on, allowing for proactive solutions before malfunctions occur. This approach is beneficial as it enables planning for downtime, preparing necessary replacement parts, and scheduling maintenance in advance. To implement condition monitoring, it's crucial to identify key data points that indicate the health of the machines. Once identified, this data can be transmitted and processed using various technologies like wired, wireless, cellular connections, or indirect methods. This process helps in recording, storing, analyzing the data, and taking preventive actions as needed.

In simpler systems where failures have minimal impact, reactive maintenance is sufficient, characterized by using machinery to its limits and repairing only after failures occur. Conversely, complex systems with extensive machinery or high-risk consequences necessitate proactive maintenance. This approach involves regular inspections and preventive measures to detect and address potential issues before they lead to failures. One of the big challenges in this approach is to determine when to do maintenance. By scheduling maintenance early, the useful machine life is being wasted. By predicting when the machine failure will occur, the schedule maintenance could be scheduled before the failure. Condition monitoring helps to continuously monitor the electric machine to predict failure and schedule the maintenance as required.

There are multiple methods available to identify faults in electrical machines, including Motor current signature analysis, Park vectors, monitoring Stator voltages, Temperature monitoring, vibration analysis, and Harmonic analysis of motor torque and speed. These techniques can be categorized into two types: invasive, requires direct access to the internal components of a system or equipment, and non-invasive, monitoring and assessment of equipment without disrupting operations or physically altering the system. Motor current signature analysis, for instance, falls under the non-invasive category of condition monitoring techniques. It utilizes the input current of an induction machine to detect and diagnose abnormalities and faults related to the machine's operation.

1.2 Problem Statement

Electric machines are being used as the heart of many processes. But, no matter how robust a machine is, it is prone to failure at some point of its lifetime leading to costly repairs and maintenance. Although deterioration is inevitable, early detection of anomalies and faults will help to reduce costs due to unplanned failures and unnecessary maintenance. Similar equipment may fail sooner than the other due to differences in their loading conditions.

This research aims to use condition monitoring techniques to detect the broken rotor bar faults in squirrel cage induction machine before it escalate to catastrophic failure. Also, the dissertation aims to analyze the the effects of different loading conditions on condition monitoring of the induction machine.

1.3 Objectives

The main objective of this research work is to study the effects of the different loading conditions on the condition monitoring of an electrical machine. To achieve the main objective a condition monitoring algorithm is to be developed to detect a fault in its early stages before they lead to a catastrophic failure.

For this research work, squirrel cage induction machines with various degrees of broken rotor bars faults are being considered. The machine is also subjected to various loading conditions.

1.4 Scope

- Develop the frequency spectrum of input current signal for various motor states and loading condition.
- Extract the side band frequencies and their magnitude.
- Develop a machine learning model which can differentiate between various machine states.
- Evaluate the performance of the model at various loading condition.

1.5 Limitation

- Only the squirrel cage induction motor with zero to three consecutive broken rotor bar fault is analyzed.
- The developed algorithm is unable to differentiate between machine states at no load condition.
- Further validation is required for real world industrial use.

1.6 Thesis Organization

The dissertation is organized into five chapters. This section enlists a brief outline of each chapter and its contents.

- This chapter gives brief introduction of the dissertation. The problem statement is described and followed by the objectives of the thesis.

- Chapter 2 explores the necessary literature review done for this dissertation including the fundamentals of induction machine, condition monitoring, and machine learning theory. This chapter justifies the detection of broken bar faults in an induction machine by explaining the effects of the fault on the operation of the machine.

- Chapter 3 describes the research methodology of the dissertation including the experimental setup and workflow.

- Chapter 4 discusses the obtained results and performs the analysis of the trained network on the test data set.

- Chapter 5 concludes the thesis work.

Finally, this thesis will end with a list of references and the relevant appendices.

CHAPTER TWO: LITERATURE REVIEW

This chapter explores the necessary literature review done for this dissertation. It covers the fundamentals of induction machine, its operation and faults, condition monitoring techniques, and machine learning theory.

2.1 Induction Machine

The induction machine operates as both a generator and a motor, though its applications vary significantly in each role. As a generator, it generally exhibits lower performance compared to synchronous machines, primarily due to factors such as voltage regulation and frequency control challenges. The three-phase induction machine is widely adopted as a primary drive in various industrial and commercial applications. The popularity induction machine as a motor stems from several key advantages. Firstly, induction motors are renowned for their cost-effectiveness, a simple design that lacks brushes and commutators, thereby reducing maintenance needs. This simplicity also contributes to their robustness and reliability, making them suitable for continuous operation in harsh environments. The most common type of induction machine is the squirrel cage machine and consumes around 85% of power in industrial application[3].

2.1.1 Construction

The motor comprises two main components housed within a frame: the stator and the rotor. The stator remains stationary and is typically made of laminated steel sheets. These sheets are designed to reduce eddy current losses caused by the changing magnetic fields. Inside the stator, there is a winding made up of three separate phases of electrical conductors. When an alternating current passes through these windings, it creates a magnetic field that rotates around the stator. The rotor is the rotating part of the motor. Rotors can be classified as wound rotor or squirrel cage rotor. The squirrel cage rotor is the most widely used rotor type. The core of the rotor is typically cylindrical and made of stacked laminated steel sheets. These laminations are insulated from each other to reduce eddy current losses. Embedded within the rotor core are conductive bars or “squirrel cage” conductors, often made of aluminum or copper. These bars are typically placed in slots that are cut into the rotor core, running parallel to the axis of the rotor. The exploded view of the squirrel cage induction motor is shown in Figure 2.1[4]

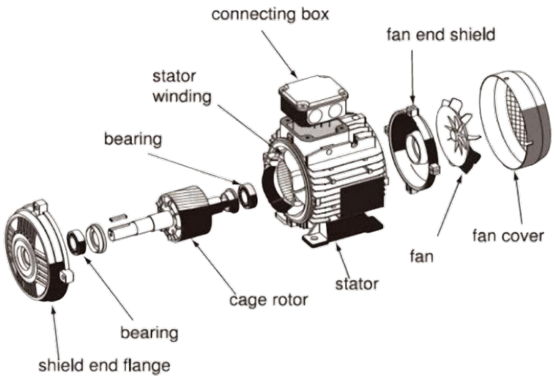

Figure 2.1: Squirrel Cage Induction Motor Exploded View[4]

2.1.2 Operation

The operation of the induction machine relies on electromagnetic induction. In an induction machine, the stator plays a crucial role. It contains a three-phase winding, which is designed to receive a three-phase AC electrical supply. When this three-phase supply is applied to the stator windings, it generates a rotating magnetic field within the machine's air gap. This rotating magnetic field has a constant amplitude and a constant speed of rotation which is given by

$$N_s = \frac{120p}{f},$$

where p is the number of poles and f is the supply frequency.

This rotating magnetic field induces an electromotive force in the rotor conductors as they cut through the magnetic field. Since the rotor conductors are short-circuited, current flows through them due to the induced emf. The interaction between this induced current and the rotating magnetic field generates a magnetic force. According to the principles of electromagnetism, this force acts perpendicularly to both the magnetic field and the direction of current flow in the rotor conductors, resulting in the production of torque. This torque causes the rotor to rotate, driving the mechanical load connected to the motor shaft. Thus, the induction motor harnesses the interaction between magnetic fields and induced currents to produce rotational motion and perform mechanical work efficiently.

2.1.3 Induction Machine Faults

Induction machines are susceptible to different types of faults during their operation, which can be categorized into two main groups: electrical and mechanical faults. The following Table 2.1 summarizes the induction machine faults.

Table 2.1: Induction Machine Fault Classification

Class	Causes	Example
Electrical	Overloading of the machine for extended duration, poor ventilation, contamination, excessive vibration	Broken rotor bar, broken rotor end, inter or intra turn short circuit, phase to ground short circuit, unbalanced voltage supply, open circuit faults
Mechanical	Manufacture imperfections, inappropriate settlement of lubrication, improper bearing installation,	Bearing faults, uneven air-gap eccentricity, shaft misalignment

Many of these faults typically begin as minor deviations from normal operating conditions. If left untreated during the early stages, they have the potential to escalate into severe failures. The Table 2.2 shows major motor components along with their failure percentages from various surveys.

Table 2.2: Major Motor Component Failure Percentage

Major Motor Components	**Failure Percentage**		
	IEEE – EC[5]	***IEEE – IAS[6]***	***IEEE – IAS[7, 8]***
Stator	36	16	26
Bearings	41	51	44
Rotor	9	9	8
Others	14	28	22

This dissertation focuses on broken rotor bar faults in a squirrel cage induction machine. While these faults constitute approximately 10% of all failures, their severity can vary significantly and potentially lead to complete motor failure[3]. Broken rotor bar faults occurs when one or more rotor making up the cage breaks partially or completely.

2.1.4 Causes of Broken Rotor Bar Faults

Broken rotor bar faults occur when one or more of the bars that make up the rotor partially or completely breaks. The failure is caused by the combination of one or more of the following[9, 10].

- **Overheating of the rotor cage**:
  This can occur from direct on-line starting or continuous overloading of the machine, stressing the motor's components and potentially leading to damage or reduced lifespan.

- **Mechanical stress**:
  This includes pulsating loads, unbalanced loads, bearing failures, excessive vibrations, and voltage fluctuations, all of which can impact the mechanical integrity of the motor and its associated components.

- **Magnetic stress**:
  This refers to unbalanced electromagnetic forces within the motor, which can lead to mechanical vibrations, noise, and potential damage if not properly monitored or controlled..

- **Contamination and corrosion**:
  Exposure to chemicals or moisture can lead to corrosion of motor parts, affecting performance and potentially causing failures if not addressed.

- **Manufacturing defects**:
  Issues originating from the manufacturing process, such as material flaws or assembly errors, can impact motor reliability and longevity..

2.1.5 Effects of Broken Rotor Bar Faults

A broken rotor bar carries minimal or no current depending on the degree of the fault. This causes rotor current to be unbalanced[11]. A motor can operate in this asymmetrical condition but results in unbalanced air gap flux, increased losses, increased torque oscillations and decrease in average torque[12]. Due to increase in losses and decrease in average torque, the motor slip increases at constant load as the severity of the fault increases. With the increase in the severity of the fault, these effects become more pronounced. Adjacent rotor bars experience higher currents because the broken bar cannot conduct its original current flow. Figure 2.2[13] illustrates the current density distribution in a squirrel cage induction motor under healthy and faulty conditions, highlighting increased current density near the broken bar as the fault worsens. This rise in current results in elevated rotor temperatures and increased losses, as heat loss is proportional to the square of the current. This increased temperature of the rotor bar causes the rotor to expand and thus increases the tension in the bar. Higher temperatures, electrical stress, and mechanical stresses can deform the rotor over time, increasing the likelihood of adjacent rotor bar failures and can then escalate to other rotor bars.

In the motor with the high rotor speed, the broken rotor bar may experience sufficient centrifugal forces and can bend toward the stator. This rotor bar may then come in contact with the stator winding leading to the motor failure[14].

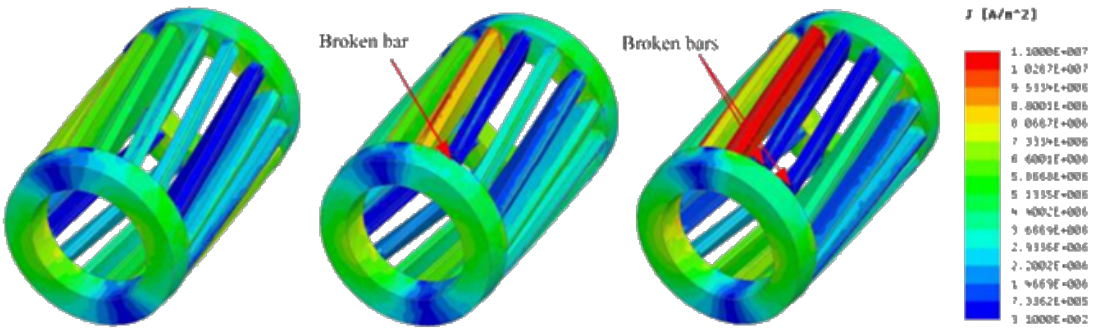

Figure 2.2: The current density distribution of squirrel cage machine at healthy and faulty condition[13]

2.2 Condition Monitoring

Assessing the condition of electrical machines through continuous monitoring involves evaluating their operational status to detect faults early and schedule maintenance effectively, with the intention of preventing catastrophic failures. The process involves regular evaluation of various parameters to determine whether the machine is operating in a healthy state, experiencing faults, or showing signs of wear. This evaluation aids in establishing a maintenance schedule. The essential steps of condition monitoring include data acquisition using sensors, preprocessing to eliminate unwanted noise and harmonics, identification of condition indicators, and training models to differentiate between different machine states. The selection of parameters to monitor depends on factors such as the type of machine, operating conditions, specific requirements, and the adopted monitoring technique

2.2.1 Need of Condition Monitoring

There are numerous faults that can threaten the operation of the machine. This faults typically starts as minor deviation in the operation and if left untreated at early stages, can escalate quickly. Condition monitoring plays a crucial role in early fault detection and serves the following purposes[2].

- Preventing catastrophic failures and extensive damage of the machines.
- Preventing unscheduled shutdowns and outages.
- Optimizing machine performance.
- Reducing repair time and spare parts inventory.

- Extending the maintenance cycle.
- Minimizing risks to life, the environment, and financial stability.

2.2.2 Condition Monitoring Techniques

Condition monitoring typically begins with basic inspections. Minor changes such as unusual heat, abnormal pressure, unfamiliar sounds, excessive vibrations, or unusual odors often indicate potential issues. However, condition monitoring techniques range from simple visual inspections to advanced technologies. Here are some of the most commonly employed condition monitoring techniques[15]:

(i) **Temperature Condition Monitoring**
Thermal overloading occurs when electrical machines operate at temperatures higher than their designed limits for extended periods and is a frequent cause of failure in electrical machines, leading to insulation deterioration, breakdown and can severely affect the integrity of the mechanical components like bearings. Therefore, monitoring temperature conditions is crucial to ensure maintain safe operational temperature limits. This involves studying of the heat and radiation pattern in machines to detect the signs of potential failure or degradation. Such monitoring helps to identify issues such as misalignment, inadequate lubrication, imbalances, wear, and mechanical stress.

(ii) **Chemical Condition Monitoring**
Electrical machine uses complex organic materials to insulate the conductor from each other and other parts of the machine. This helps to prevent electrical faults and ensure safe operation. When exposed to high temperatures, electrical and mechanical stress, and moisture they undergo chemical degradation. This produces a wide range of chemical by products in the gas, liquid, and solid states. The formation of this by products can affect the performance and safety of the machines. For example: lubrication oil are crucial for operation of mechanical components as it helps to not only reduce the friction but also dissipate heat generated during operation. Over time, lubrication oils undergo their own degradation process. They can break down chemically due to exposure to heat and mechanical stress, leading to the formation of degradation products. Additionally, lubrication oils can accumulate particles from the wear and tear of bearings and seals they are designed to lubricate and cool. These particles can further degrade the oil's performance and potentially impact the overall efficiency of the machine. To assess the condition

of an electrical machine, especially regarding the insulation materials and lubrication oils, chemical monitoring is crucial. Chemical monitoring involves detecting and analyzing the degradation products of the organic materials. By monitoring these chemical changes, allows for timely maintenance and replacement of insulation materials and lubrication oils, thereby minimizing the risk of machine failures and optimizing its performance and longevity.

(iii) **Vibration Condition Monitoring**

Vibration conditional monitoring is a widely utilized technique for diagnosing faults in an electric machine. It involves the continuous or periodic measurement and analysis of vibrations emitted by the machine. Vibration sensors, typically piezoelectric accelerometers, are used to measure vibrations generated by rotating or reciprocating machinery. Changes in vibration patterns, frequencies, or amplitudes can indicate faults such as misalignment, imbalance, bearing wear, shaft cracks, or gear tooth damage. Faults in electric machines can lead to increased mechanical and electromagnetic forces that disturb the machine's magnetic field or mechanical balance. These disturbances manifest as distinct patterns of structural vibrations observable on the machine's frame. Dedicated vibration sensors are strategically placed to monitor these vibrations, enabling early detection of faults and proactive maintenance to prevent breakdowns.

(iv) **Motor Current Signature Analysis**

Motor Current Signature Analysis (MCSA) is a widely utilized technique for non-intrusive condition monitoring of electrical machines. It involves the analysis of the frequency spectrum of the current flowing into the motor during operation. MCSA involves capturing and analyzing the current flowing through the motor's stator windings. This current contains valuable information about the motor's health and condition. The current signal is analyzed to identify its frequency components. Normal operation produces a characteristic frequency spectrum. However, when faults like broken rotor bars, air gap eccentricity, bearing issues, or faults in the stator windings occur, they cause irregularities in the current signal. These faults modulate the current signal, introducing additional frequencies known as side band harmonics. By examining the frequency spectrum for these side band harmonics and other deviations from the normal pattern, MCSA can detect the presence of specific faults in the motor. Each type of fault produces a unique pattern of side band harmonics, which can be correlated with known fault signatures to identify the type and severity of the fault. MCSA is considered non-intrusive because it does not require physical access to internal motor components. It simply monitors

the electrical signals (current) entering the motor, which are easily accessible from external monitoring points.

2.3 Detection of Broken Rotor Bar Faults

The stator input current contains the information about the machine health. The operation of the induction machine with broken rotor bar induces the line currents at the frequencies given by[12, 16]

$$\mathbf{f_{brb} = f_s(1 \pm 2s)}$$

where,
$\mathbf{f_s}$ is the fundamental component of the stator current
$\mathbf{s}$ is the motor slip

which are known as the side band components. An increment in the magnitude of theses characteristics frequency in the stator current indicates a rotor bar fault. Therefore, the study of these frequencies is a viable option to differentiate motor states. The side band $\mathbf{f_s(1-2s)}$ is termed as Left Side Band (LSB) and $\mathbf{f_s(1+2s)}$ is termed as Right Side Band (RSB). Figure 2.3 shows the measured sidebands from [17].

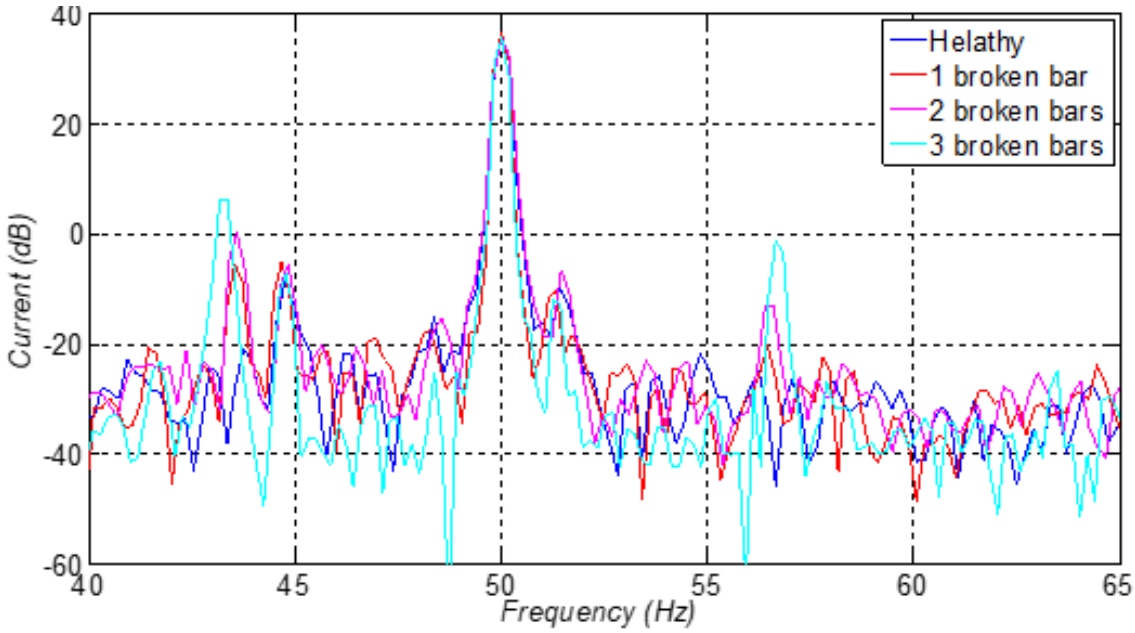

Figure 2.3: Measured side bands from [17]

2.4 Machine Learning

Machine Learning represents a subset of Artificial Intelligence focused on improving system performance through data-driven learning, employing statistical methods and algorithms akin to human learning processes. This iterative approach allows systems to iteratively enhance accuracy and functionality based on acquired experience and data inputs. Machine Learning finds extensive application across various fields, including natural language processing, speech recognition, and classification tasks among others. In practical terms, Machine Learning involves training algorithms to recognize patterns and make informed predictions or decisions without explicit programming for each scenario. By analyzing large datasets, these algorithms identify underlying patterns and relationships, enabling systems to adapt and improve over time. This adaptive capability is crucial for tasks such as understanding and generating human language, distinguishing speech patterns, or categorizing data into distinct groups. Moreover, the versatility of Machine Learning extends beyond specific domains, impacting industries ranging from healthcare to finance and beyond. Its ability to automate and optimize processes, coupled with its potential for predictive insights, makes it a cornerstone of modern technological advancements. Ultimately, Machine Learning continues to evolve, driven by ongoing research and innovation, promising further enhancements in artificial intelligence and its practical applications across diverse sectors globally. Machine learning approaches can be categorized into three main types:

(i) **Supervised Learning**

Supervised learning involves a training dataset where each example is represented by a vector of input variables and their corresponding desired outputs, organized into a matrix. The process aims to optimize a specified function—typically a loss or cost function—by adjusting model parameters iteratively. Through this optimization, the model learns to predict outputs accurately for new inputs by capturing patterns and relationships in the data. The quality of the training data, choice of objective function, and optimization algorithm are crucial for the model's ability to generalize and make reliable predictions on unseen data, making supervised learning foundational in fields like image recognition and predictive analytics. Commonly used algorithm includes support vector machines, linear regression, K-nearest neighbour, neural networks, naive Bayes, and random forest.

(ii) **Unsupervised Learning**

Unsupervised learning utilizes set of unlabeled data and identifies common features to categorize into meaningful clusters. The model then reacts on the new data sets

based on presence or absence of such features. Commonly used algorithm includes Hopfield learning, maximum likelihood, Hierarchical clustering and partial least square.

(iii) **Reinforcement Learning**

Reinforcement learning uses an interactive environment to achieve predefined goals. It explores this environment and receives feedback or rewards based on its actions, which it seeks to optimize through learning. The environment is often represented using a Markov process, allowing the agent to make decisions based on current states and actions, and enabling the modeling of dynamic interactions over time. Commonly used algorithms are Monte Carlo methods, temporal differences and state action reward state action.

2.4.1 Multi Layer Perceptron

The Multi Layer Perceptron (MLP) is an artificial neural network characterized by its feedforward structure, encompassing multiple layers such as an input layer, one or more hidden layers, and an output layer, each layer being fully interconnected. The fundamental unit of an MLP is the perceptron. The perceptron shown in Figure 2.4 takes the three values of the input vector x and evaluates the weighted sum $\sum_{i=1}^{n} x_i w_i + b$ where b is bias term added to the perceptron to provide additional flexibility in modeling complex patterns in the input data and is usually not shown in the network architecture. The activation function determines the output bases on the weighted sum.

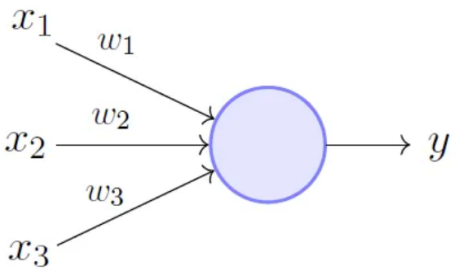

Figure 2.4: Perceptron

Some of the commonly used activation function are:

1. Sigmoid function

   The sigmoid activation function transforms real-numbered inputs into a range between 0 and 1. The sigmoid function approaches a horizontal slope at extreme input values, specifically near negative infinity or positive infinity. This phenomenon is

known as the vanishing gradient, where the gradient or slope of the function becomes exceptionally small. The sigmoid is defined as:

$$f(x) = \frac{1}{1+e^{-x}}$$

The Figure 2.5 shows the sigmoid function.

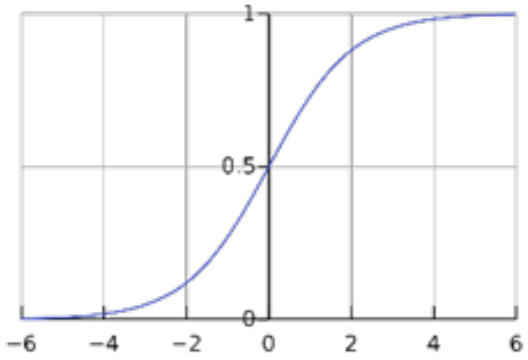

Figure 2.5: Sigmoid activation function

2. Hyperbolic tangent function
   The hyperbolic tangent function closely resembles the sigmoid activation function, sharing the characteristic S-shape and has an output range from -1 to 1. In the case of tanh, as the input increases (becomes more positive), the output approaches 1.0, while the ouput decreases (becomes more negative), the output tends towards -1.0. The tanh is defined as:

$$f(x) = \frac{e^{x}+e^{-x}}{e^{x}-e^{-x}}$$

The Figure 2.6 shows the tanh function.

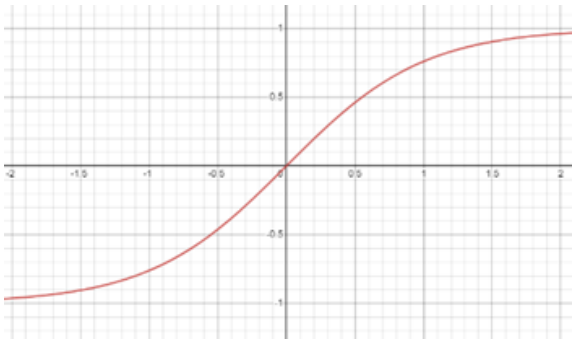

Figure 2.6: tanh activation function

3. ReLU function

   ReLU, short for rectified linear unit, transforms the input to zero or itself. It functions by outputting zero if the input is zero or negative, and retaining the input value if it is positive. Mathematically ReLU is represented as:

$$f(x) = max(0, x)$$

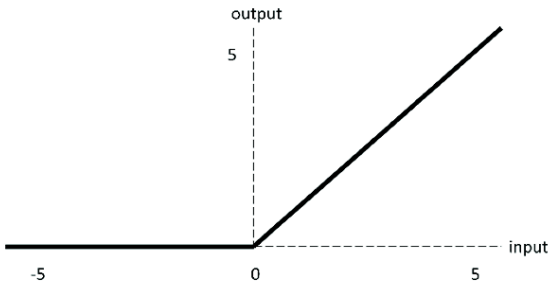

Figure 2.7: ReLU activation function

4. Leaky ReLU

   Leaky ReLU is an activation function used in artificial neural networks. It is an enhancement over the traditional ReLU function, designed to address the "dying ReLU" problem where neurons can become inactive during training due to a consistently low output. In essence, Leaky ReLU utilizes a non-zero small gradient when the input is negative, instead of simply zeroing out like ReLU. Mathematically, it is defined as:

$$f(x) = \begin{cases} x, & \text{if } x \geq 1 \\ ax, & \text{if } x < 1 \end{cases}$$

5. SoftMax

   The SoftMax is a function that turns the vector of k real values into vector of k real values that sums to 1 which can now be interpreted as probabilities. If one of the inputs is small or negative, the softmax turns that input into a small probability, and if an input is large, then it turns that input into a large probability. The softmax is defined as:

$$\sigma(x_i) = \frac{e^{x_i}}{\sum_{j=1}^{k} e^{z_k}}$$

The softmax is used as an activation for output layer of multi class classification networks.

Each layer in an MLP is composed of several perceptrons. Connecting these layers in sequence forms the MLP architecture. The width of a layer is determined by the number of perceptrons in a layer, while the network's depth is defined by the total number of these interconnected layers. The output layer, located at the final stage of the network, is responsible for producing the desired output. An MLP with four layers, one input layer with four perceptrons, two hidden layers with five and three perceptrons, and output layer with two perceptrons is shown in Figure 2.8.

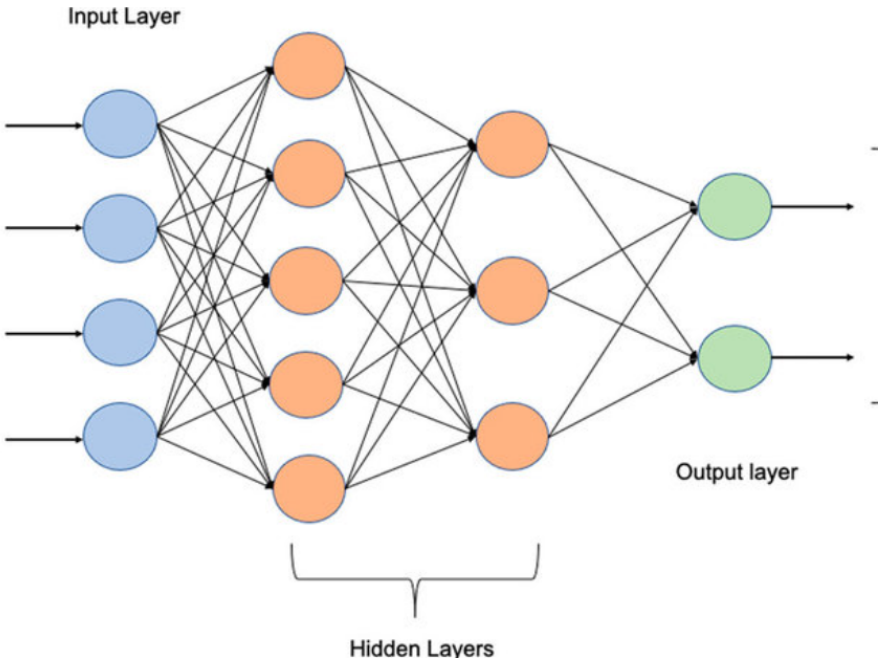

Figure 2.8: MLP with two hidden layers

For, the above MLP, if each layer transform the input via function f_1, f_2, f_3, f_4, respectively from input to output layer. Then for an input vector x, the output vector will be $f_4(f_3(f_2(f_1(x))))$.

Learning in MLP involves the iterative adjustment of connection weights between neurons, a process critical for the network to learn patterns and relationships from data. This research focuses on supervised learning, where the network learns from labeled examples, supported by the Adam optimizer for efficient weight updates. In supervised learning with an MLP, each training cycle begins by presenting an input vector to the network. The network processes this input through its layers of neurons to produce an output vector. This output is then compared to the expected output, known as the target output. The comparison between the network's output and the target output generates an error signal, which

quantifies the disparity between the predicted and desired outcomes. This error signal serves as a guide for adjusting the weights of the network connections. The Adam optimizer facilitates this adjustment process by efficiently updating the weights based on the error signal, aiming to minimize prediction errors over time. Throughout training, the network repeatedly adjusts its weights in response to observed errors, gradually improving its ability to accurately map inputs to outputs. This iterative learning process continues until the network achieves the desired level of accuracy on the training data, enabling it to generalize well to new and unseen data. In summary, supervised learning in neural networks involves optimizing connection weights through error minimization, facilitated by algorithms like Adam, to enhance the network's predictive capabilities and performance.

CHAPTER THREE: METHODOLOGY

This chapter describes the workflow of the research starting from the data acquisition, extraction of characteristic frequency and its magnitude from the measured current signal, and culminating with the MLP model to differentiate between the various motor states.

3.1 Approach

At first to understand the concepts, needs and the development of fault diagnostics and condition monitoring techniques, a literature review is done. The data is then collected from the experimental setups at Aalto University, Finland and Tallin University of Technology, Estonia. To extract the features of the measured signal, discrete Fourier Transform (DFT) is performed. Then, neural network is trained to detect the faults using the extracted features. Finally, the documentation is done. The overall methodology that has been utilized in this dissertation is shown in Figure 3.1.

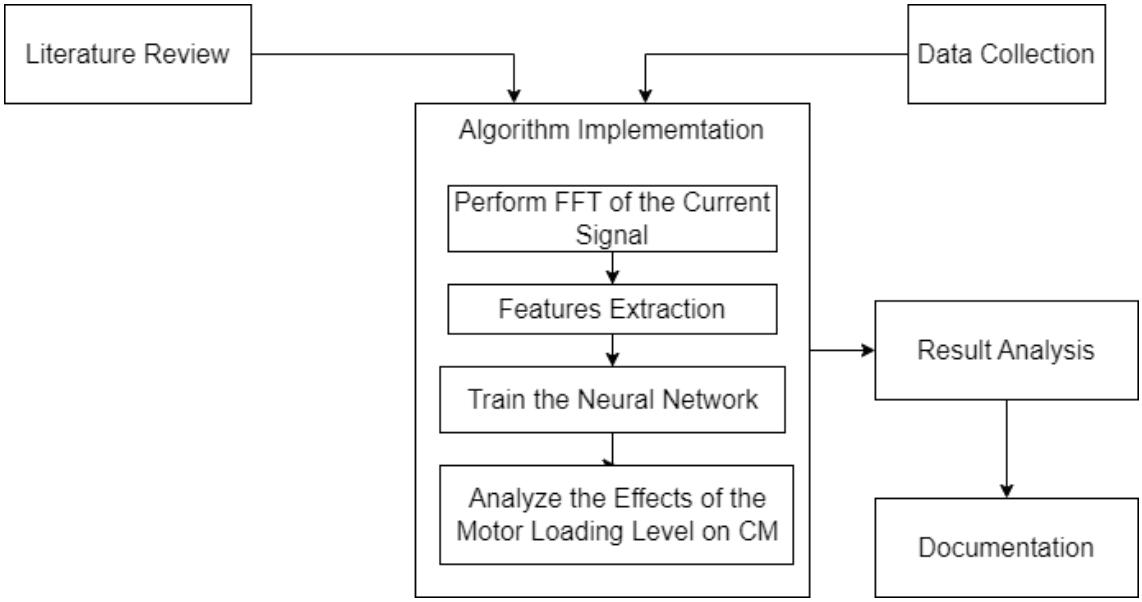

Figure 3.1: Methodology Approach

3.2 Tools and Software

This section lists the tools and software used in this dissertation.

3.2.1 Microsoft Office

Microsoft Office comprises a suite of software applications created by Microsoft, including a word processing program (Word), a spreadsheet application (Excel), and a presentation software (PowerPoint), among other tools. In this dissertation, Word is utilized for initial report drafting, while Excel is employed for storing the extracted features.

3.2.2 Matlab

Matlab is a software platform for programming and numerical computing, created by MathWorks. In this research, Matlab is utilized to apply the Fourier transform to the measured current signal, extracting the frequency and magnitude of the sidebands

3.2.3 Kaggle

Kaggle is a data science platform and online community owned by Google. It includes a range of Python libraries utilized for data science and machine learning purposes. The Table 3.1 shows the various libraries used in this dissertation.

Table 3.1: Python Libraries Used

Libraries	**Purpose**
Numpy	Array manipulation and matrix processing
Pandas	Data manipulation and analysis
Matplotlib	Data visualization and plotting
Seaborn	Data visualization and plotting
Scikit Learn	MLP modeling
TensorFlow	MLP modeling
Keras	MLP modeling

3.2.4 Overleaf

Overleaf is an innovative online platform and LaTeX editor designed specifically for academics, researchers, and professionals involved in scientific writing and publishing. Overleaf provides a collaborative environment where users can create, edit, and manage LaTeX documents seamlessly, without the need for local LaTeX installations or complex setup. It offers LaTeX templates from various reputable journals. In this dissertation, overleaf is used for preparing the reports.

3.3 Data Acquisition

This section describes experimental procedures carried out by the team of Aalto University, Finland and Tallin University of Technology, Estonia. The data obtained from the experiment is used as the basis for this research.

3.3.1 Experimental Setup

The experimental setup involves two identical motors connected back-to-back via their shaft: the first healthy motor is used to load the test machine which had 0 to 3 broken rotor bar (BRB)s. Both the motors were controlled by a variable frequency drive. The Dewetron transient recorder is used to record the stator currents at the sampling rate of 20 kHz for about 20 seconds after steady operation. The experimental setup is shown in Figure 3.2 and the schematic diagram is shown in Figure 3.3. The machine specification is shown in Table 3.2.

Figure 3.2: Experimental Setup

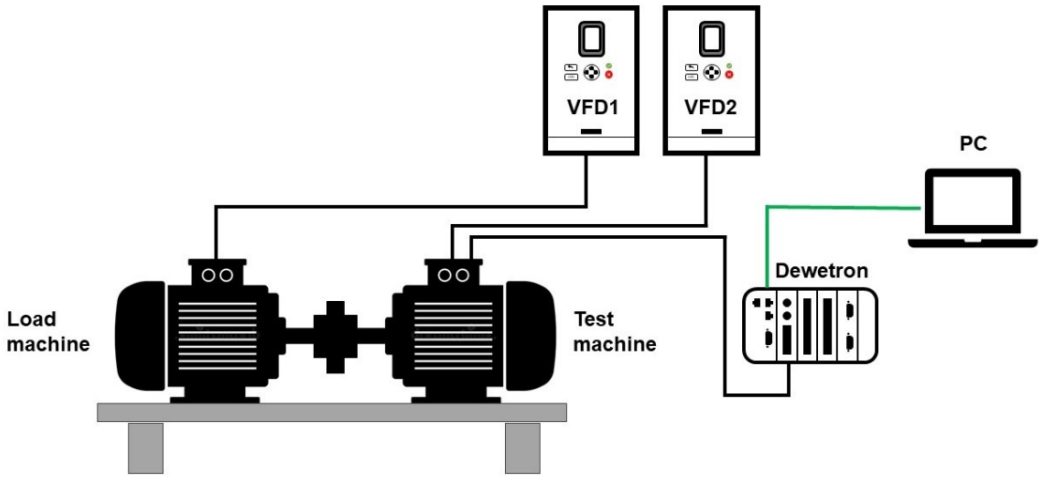

Figure 3.3: Schematic Diagram of the Setup

Table 3.2: Machine Specification

Parameters	Symbols/Units	Value
Number of poles	P	4
Number of Phases		3
Connection		Δ
Voltage	V	400
Current	A	15.3
Power	kW	7.5
Speed	rpm	1460
Power factor	cos ϕ	0.79

3.3.2 Experimental Procedure

The experiment was carried out as below:

- The test machine steady phase current was recorded for 20 seconds after steady state under healthy rotor conditions (i.e., at 0 BRB fault) at different load levels of 0, 25, 50, 75, and 100 percent of the rated nominal load at the sampling rate of 20 kHz.
- The BRB was realized by drilling a hole in the rotor slot.
- The bars were broken sequentially, and the current signal recordings were obtained for 1, 2, and 3 BRBs state.
- The recordings were stored in a .mat file.

The BRBs made during the experiment are shown in Figure 3.4.

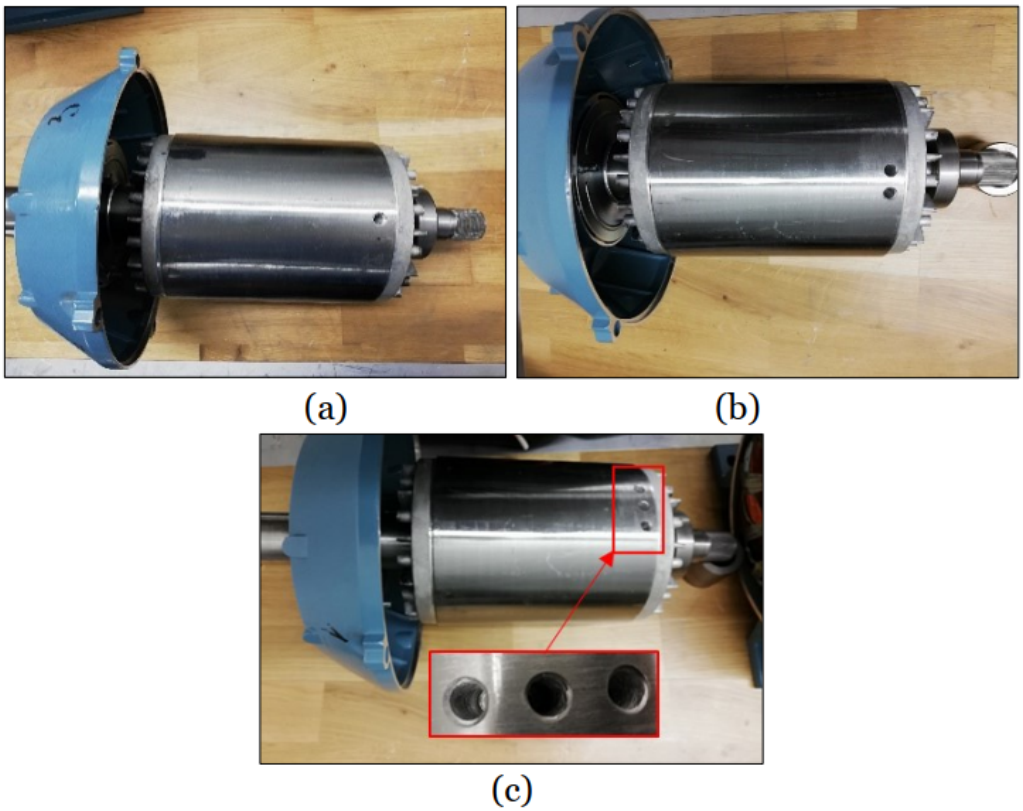

Figure 3.4: Rotor with (a) one, (b) two and (c) three BRBs

The example plot of the recorded current signal is shown in Figure 3.5, Figure 3.6, and Figure 3.7.

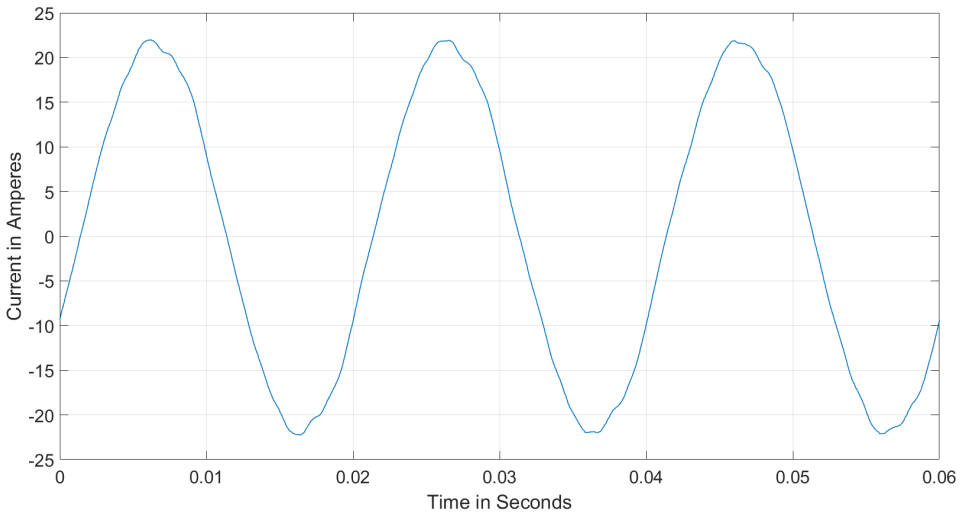

Figure 3.5: Current Profile for Healthy Case at 100% Load

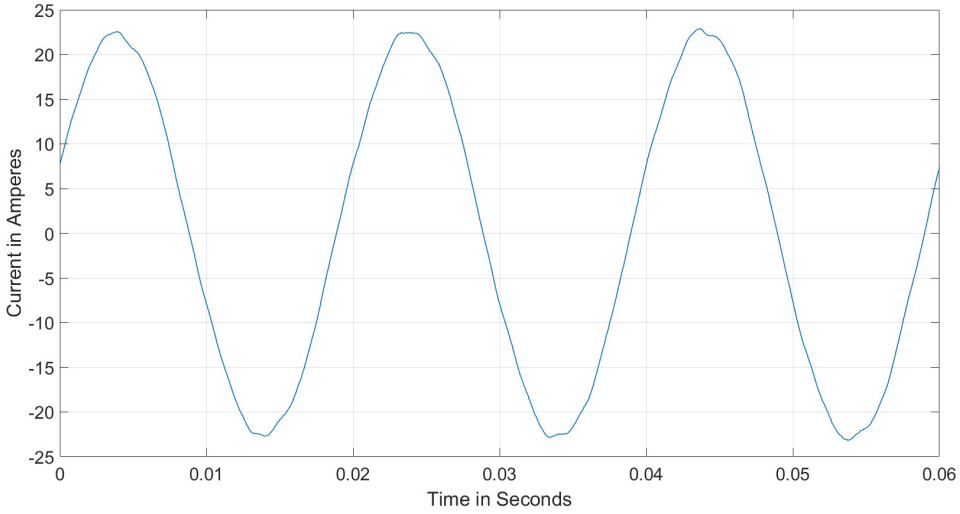

Figure 3.6: Current Profile for 2 BRB Case at 100% Load

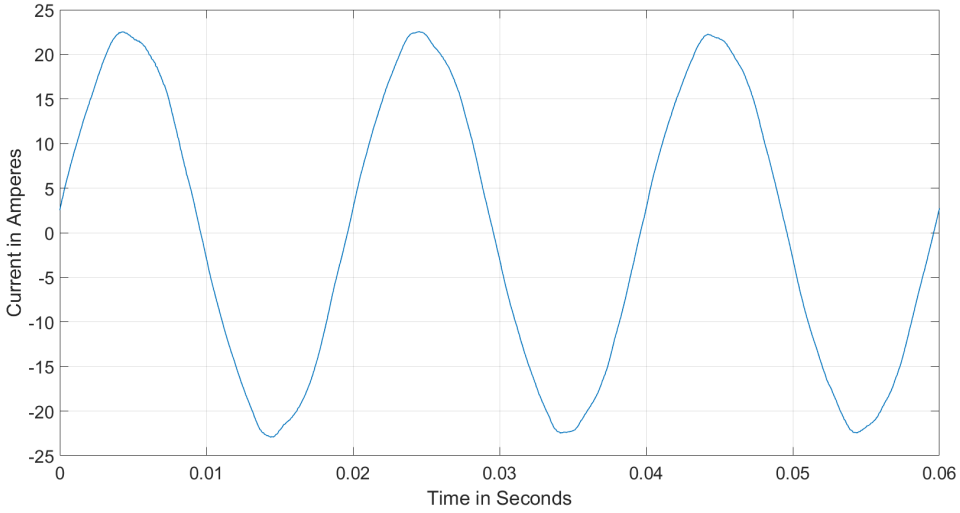

Figure 3.7: Current Profile for 3 BRB Case at 100% Load

From Figure 3.5, Figure 3.6, and Figure 3.7, it can be seen that the machine states are difficult to differentiate based on time domain signal. Hence, the frequency spectrum was obtained by applying the Fast Fourier Transform (FFT) to the measured current signal.

3.4 Features Extraction

To extract the features from the measured current signals, a window of 50 electrical cycles was taken. As the current signal had a frequency of 50 Hz, the window length was equal to one second. The features obtained from this window makes up a single data point. To obtain the next data point the window was shifted by 2 electrical cycles (i.e., 0.04 seconds). This process was carried on to obtain 400 data points for a single machine state at a given loading. This process is shown in Figure 3.8.

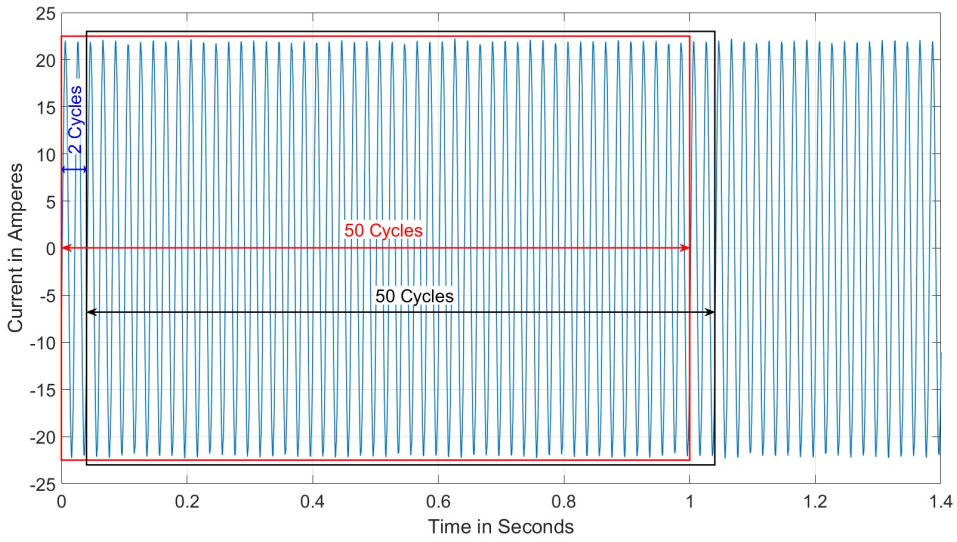

Figure 3.8: Current Signal Windowing

To transform the window into frequency domain (FFT) was used. To reduce spectral leakage, the Hann window function was employed.. The Hann window is defined as:

$$w(n) = 0.5\left(1 - cos(2\pi\frac{n}{N})\right)$$

A Hann window was used in this dissertation which is shown in Figure 3.9.

The sample current signal after Hann windowing is shown in Figure 3.10.

The Hanned current signal was then transform into the frequency domain using FFT. The FFT is described here:

Let x_n be a sequence of the N measured values.

$$x_n = x_0, x_1, x_2, ..., x_{N-1}$$

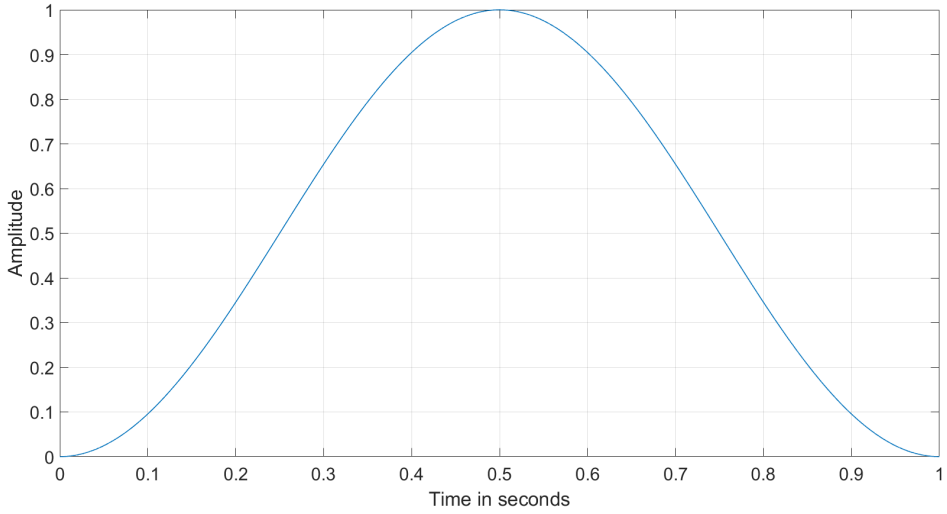

Figure 3.9: Hann Window

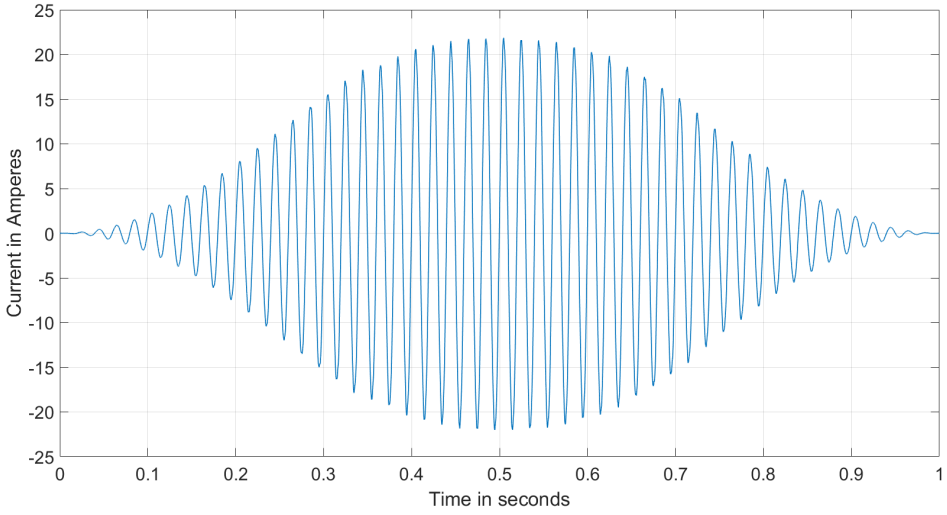

Figure 3.10: Current Signal after Hann Windowing

Then the FFT of the sequence x_n is defined as

$$X_K = \sum_{n=0}^{N-1} e^{-\frac{j2\pi Kn}{N}}$$

where $X_K = X_0, X_1, ..., X_{N-1}$ is the FFT of the sequence x_n and j is the square root of negative one, i.e., the imaginary unit. After this, the frequency and magnitude of the LSB and RSB from the frequency spectrum were taken as the features.

In total 6,400 data points were obtained, 400 points for each Healthy and Faulty state at the loading of 25, 50, 75, and 100 percent of the rated load. No Features could be extracted for no load conditions.

3.5 Multi Layer Perceptron

An MLP with three hidden layers was developed in Kaggle using libraries TensorFlow and Keras. The model consisted of five layers overall comprising input, output and three hidden layers. The input layers had four perceptrons corresponding to the number of inputs, standardized the features value to scale one. The output layer had four perceptrons, each corresponding to one of the machine state. Since, the problem is a classification type, the activation function in the final layer was set to Softmax. The hidden layers had 128, 64, and 16 perceptrons respectively with Sigmoid activation.

The MLP model was trained with Adam optimizer with the metric Accuracy and loss Sparse Categorical Cross-Entropy. The maximum number of epoch was set to 128 and batch size 32. The MLP was able to attain accuracy of 96% on the train data set. The confusion matrix was employed to access the performance of the MLP on the test dataset at various load levels which shown in Chapter 4.2.

CHAPTER FOUR: RESULTS AND DISCUSSION

This chapter presents the results obtained using the methodology described in Chapter 3.

4.1 Features Extraction

To extract the frequency and magnitude of the side bands of the measured current signal, FFT is used. Figure 4.1 to Figure 4.5 show the FFT of the measured current signal at various load levels, and at various motor states. Table 4.1 to Table 4.4 shows the magnitude and the frequency of the sidebands at different machine states. The variation of the sidebands is shown in Figure 4.7 and Figure 4.8. The FFT analysis was unable to identify sidebands in both healthy and faulty states of the motor under no-load conditions. This limitation arises because the fundamental component of the current signal is very small during no-load conditions, and the sidebands closely overlap with this fundamental component. Detecting faults in the induction machine using the magnitude and position of these side bands is feasible, as discussed in Chapter 4.2

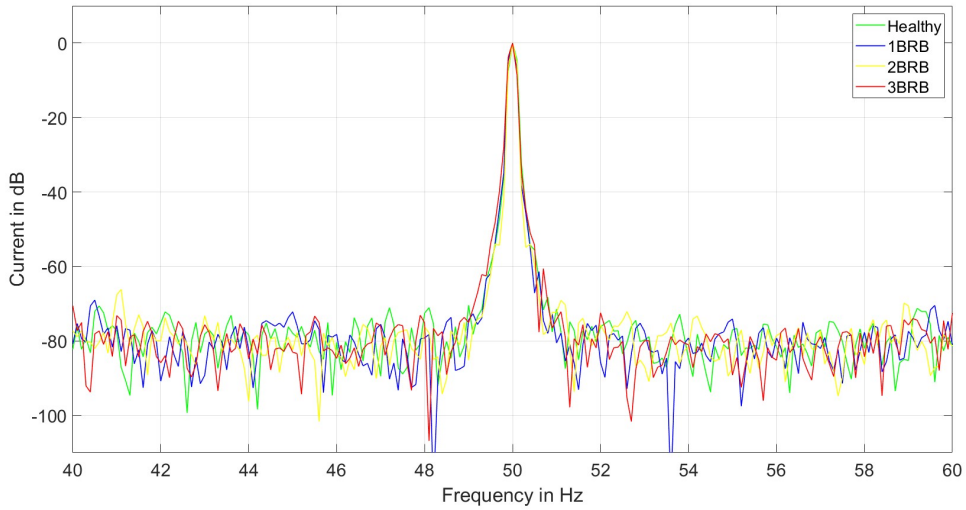

Figure 4.1: FFT of measured current signal at no load

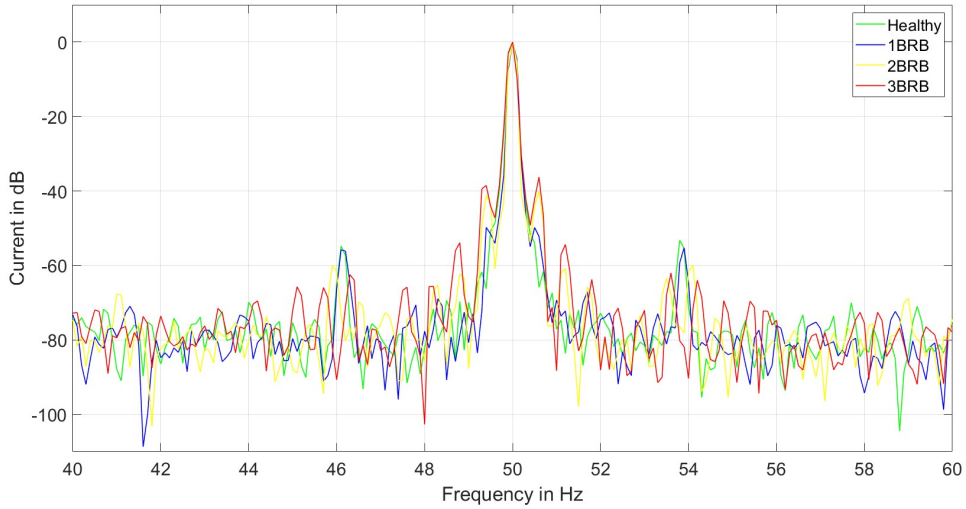

Figure 4.2: FFT of measured current signal at 25% of rated load

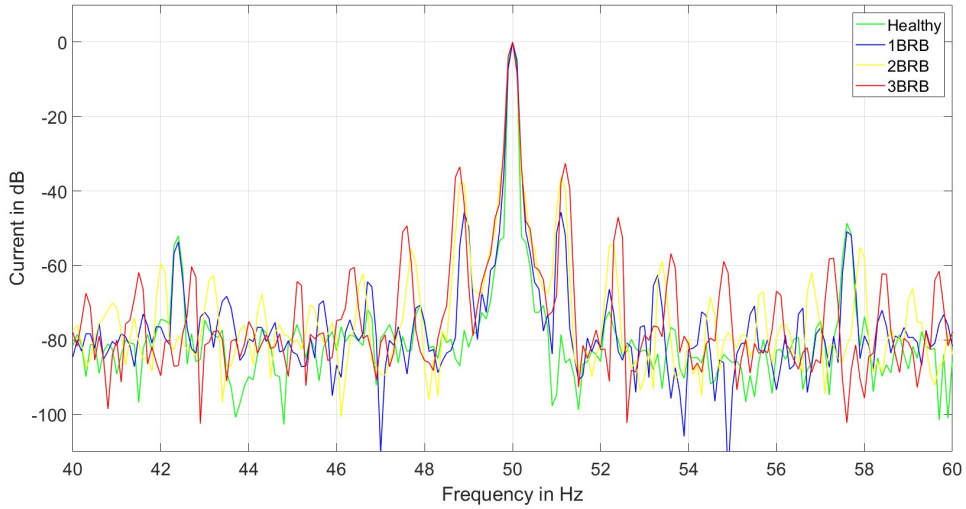

Figure 4.3: FFT of measured current signal at 50% of rated load

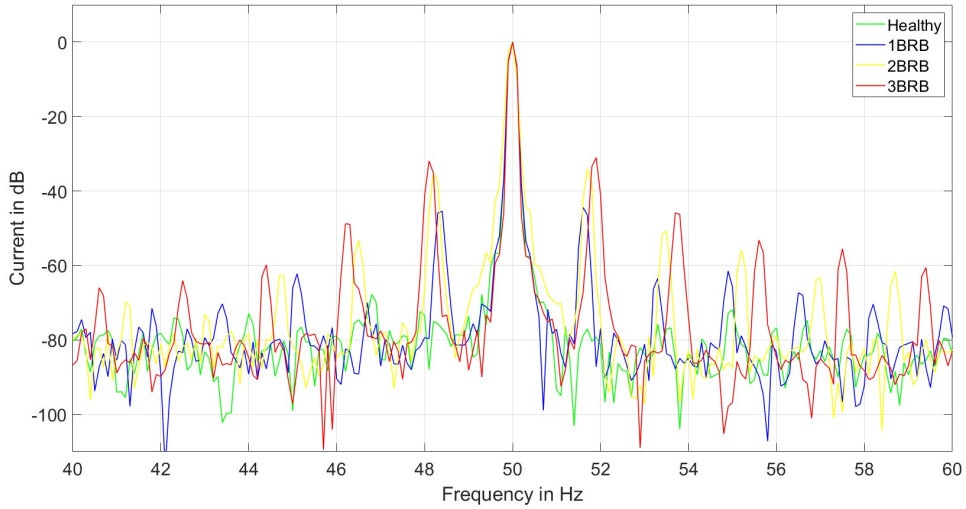

Figure 4.4: FFT of measured current signal at 75% of rated load

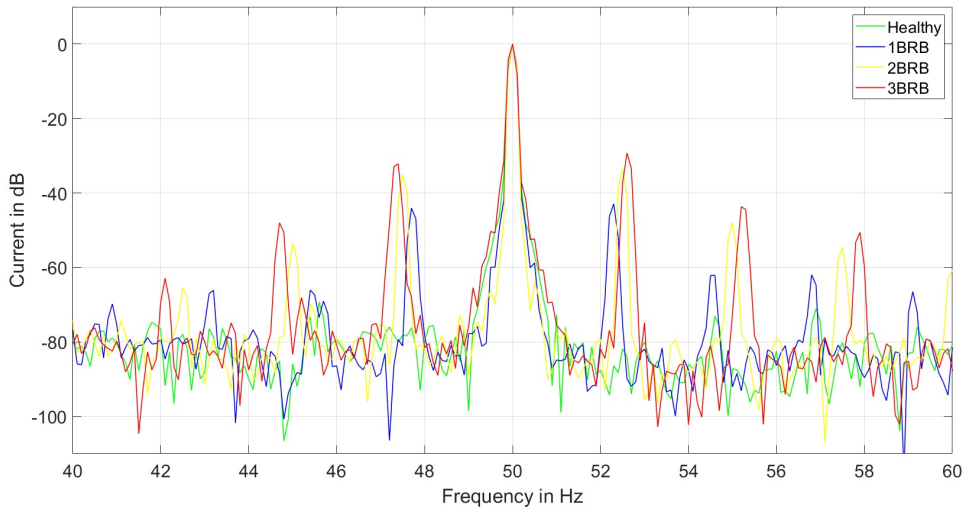

Figure 4.5: FFT of measured current signal at 100% of rated load

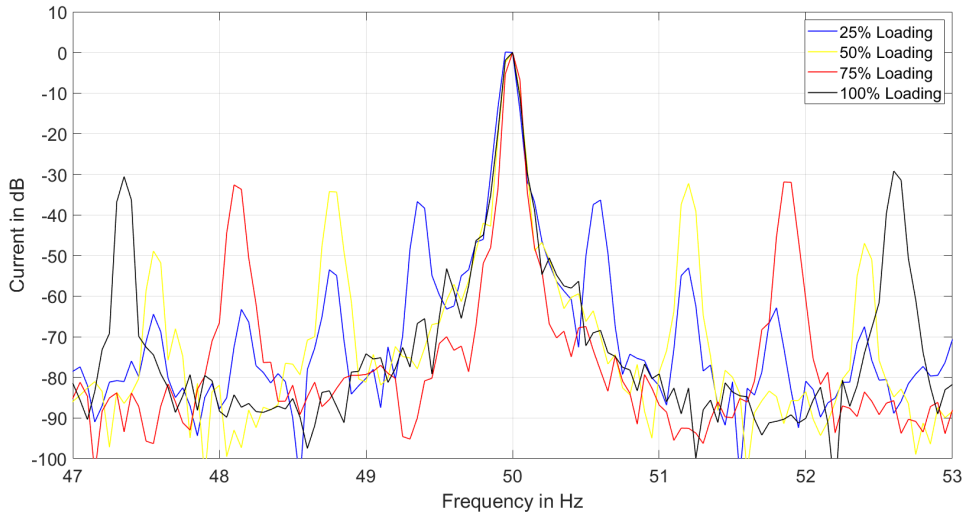

Figure 4.6: Shift in the position of side bands for 3 BRB state

Table 4.1: Side bands for Healthy State

% Loading of Rated Load	Left Side Band		Right Side Band	
	Freq. (Hz)	Mag. (dB)	Freq. (Hz)	Mag. (dB)
25	49.5	-50.74	50.5	-53.85
50	49.3	-72.59	50.7	-70.72
75	48.8	-78.68	51.2	-78.27
100	48.1	-75.82	51.8	-81.33

Table 4.2: Side bands for 1 BRB State

% Loading of Rated Load	Left Side Band		Right Side Band	
	Freq. (Hz)	Mag. (dB)	Freq. (Hz)	Mag. (dB)
25	49.4	-49.76	50.5	-49.78
50	48.9	-44.39	51.1	-45.69
75	48.4	-45.39	51.6	-44.36
100	47.7	-44.04	52.3	-42.91

Table 4.3: Side bands for 2 BRB State

% Loading of Rated Load	Left Side Band		Right Side Band	
	Freq. (Hz)	Mag. (dB)	Freq. (Hz)	Mag. (dB)
25	49.4	-41.09	50.6	-40.03
50	48.8	-37.83	51.1	-37.61
75	48.4	-35.19	51.6	-34.11
100	47.7	-35.03	52.3	-33.52

Table 4.4: Side bands for 3 BRB State

% Loading of Rated Load	Left Side Band		Right Side Band	
	Freq. (Hz)	Mag. (dB)	Freq. (Hz)	Mag. (dB)
25	49.3	-36.72	50.6	-36.32
50	48.8	-34.25	51.2	-31.22
75	48.1	-32.60	51.9	-31.89
100	47.4	-30.57	52.6	-29.19

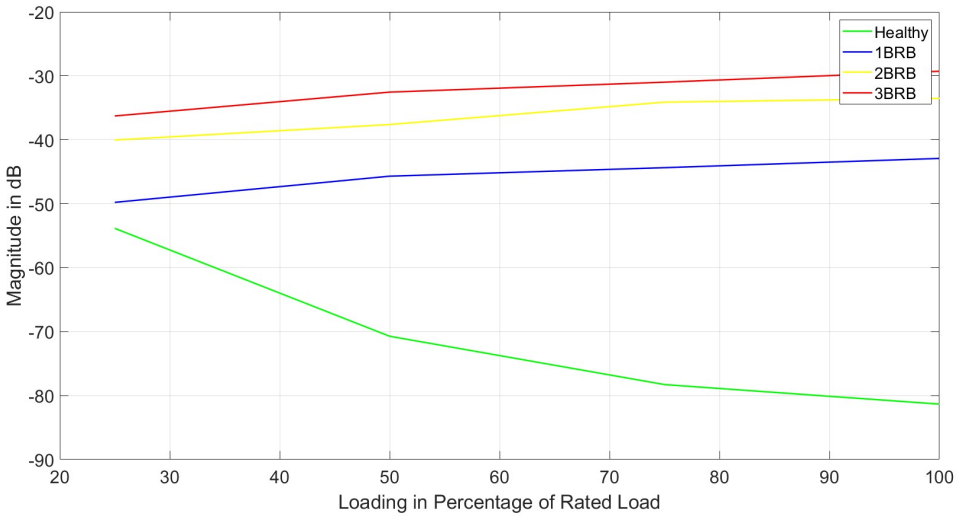

Figure 4.7: Variation of RSB with Loading

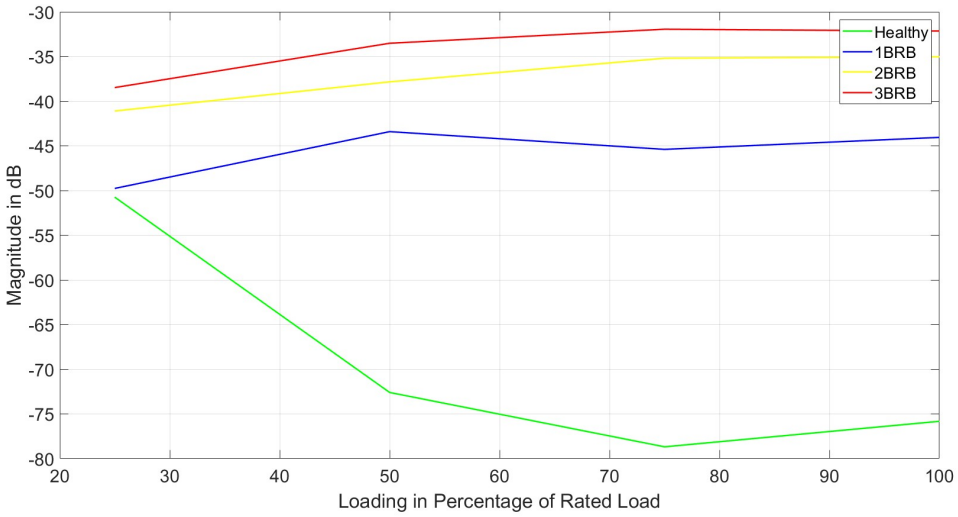

Figure 4.8: Variation of LSB with Loading

The major findings from this figures is listed below.

- **Shift in location of the side band with machine state**:
  As the severity of the fault was increased, the side band frequency shifted further away from the fundamental component. This can be attributed to the fact that, the machine losses increases with the increase in severity of the fault. The machine slip will then increase to accommodate for the increase in power demand. This is visible in Figure 4.1 to Figure 4.5.

- **Shift in location of the side band with loading**:
  As the loading of the machine was increased the side band was found to shift further away from the fundamental component. This is due to the fact that as the loading of the machine was increased, the slip of the machine increased to increase the output torque. The side band frequency given by $f_{brb} = f_s(1 \pm 2s)$ then shifts accordingly. This is shown for the case of 3 BRB motor state in Figure 4.6.

- **Variation of side band amplitude with machine state**:
  The amplitude of the side band at either side of the fundamental component was found to increase with the increase in the severity of the fault. This is shown in Figure 4.7 and Figure 4.8.

4.2 Fault Detection and Performance of the MLP

An MLP was trained to detect the fault from the measured current signal. The MLP was trained using 4800 data points and tested using 1600 data points. The test data set consists of 100 data points for a machine state at a given load level. Confusion matrices were implemented to visualize the performance of the MLP. Figure 4.9 to Figure 4.13 shows the confusion matrix of the test data set at various load levels. Table 4.5 and Figure 4.14 compares the BRB fault detection by the model at various load levels using the metrics: accuracy, precision, recall, and f1 – scores. The used terms are defined as below.

Accuracy: Accuracy assesses the ratio of correctly predicted instances. It encompasses both true positives and true negatives, among all instances examined. It provides a comprehensive evaluation of the model's overall performance across all classes, indicating how well it correctly identifies instances regardless of class distinctions. A higher accuracy score indicates that the model effectively predicts instances correctly, reflecting its

ability to generalize well to unseen data. It is calculated as

$$Accuracy = \frac{TN + TP}{Total\ Observation}$$

Precision: Precision measures the model's accuracy in predicting positive instances by calculating the ratio of true positives to the sum of true positives and false positives. It reflects the model's ability to identify relevant positive instances accurately, emphasizing the precision of its predictions. A higher precision score indicates that the model selects fewer false positives relative to true positives, demonstrating its capability to minimize incorrect positive predictions and enhance the reliability of positive classifications. It is calculated as:

$$Precision = \frac{TP}{TP + FP}$$

Recall: Recall measures the model's effectiveness in identifying all true positives within the dataset. It is calculated as the ratio of true positives to the sum of true positives and false negatives. This metric indicates how well the model sensitively detects positive instances, demonstrating its ability to correctly capture relevant examples from the dataset. It is calculated as:

$$Recall = \frac{TP}{TP + FN}$$

F1 – score: The F1-score is calculated as the harmonic mean of precision and recall, offering a single metric that harmonizes both measures effectively. It is especially useful when there is a need to strike a balance between precision, which measures the accuracy of positive predictions, and recall, which gauges the model's ability to identify all relevant instances. When both precision and recall are perfect (equal to 1), the F1-score also reaches its peak of 1, indicating an ideal classifier that achieves high accuracy in predicting positives while comprehensively capturing all relevant instances in the dataset. It is calculates as:

$$F1 - score = 2\frac{Precision * Recall}{Precision + Recall}$$

where,
TP is the true positive i.e., prediction of 0 BRB as 0 BRB,
FP is false positive i.e., prediction of 1, 2 or 3 BRB as 0 BRB,
TN is true negative i.e., prediction of 1, 2 and 3 BRB as 1, 2 and 3 BRB respectively,
FN is false negative i.e., prediction of 0 BRB as 1, 2 or 3 BRB.

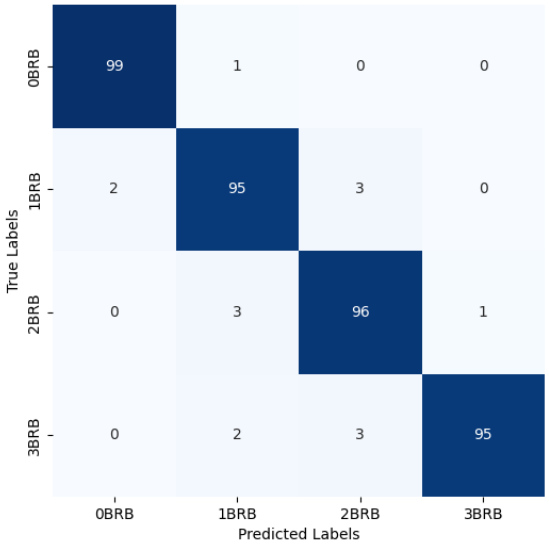

Figure 4.9: Confusion Matrix for loading level of 100% of rated load

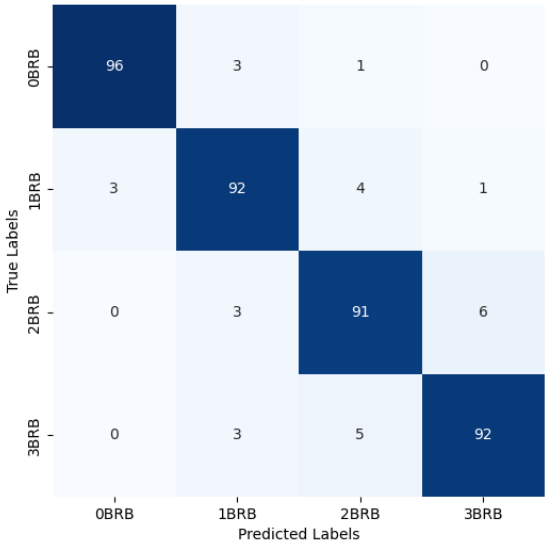

Figure 4.10: Confusion Matrix for loading level of 75% of rated load

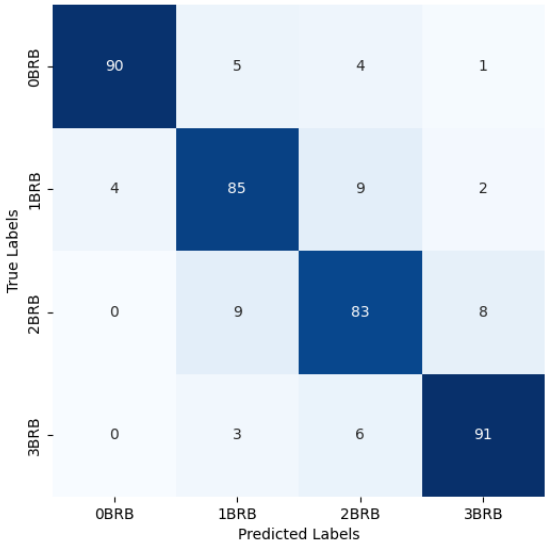

Figure 4.11: Confusion Matrix for loading level of 50% of rated load

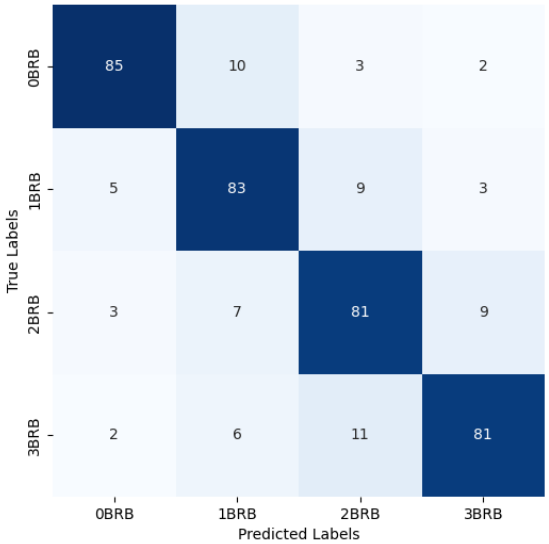

Figure 4.12: Confusion Matrix for loading level of 25% of rated load

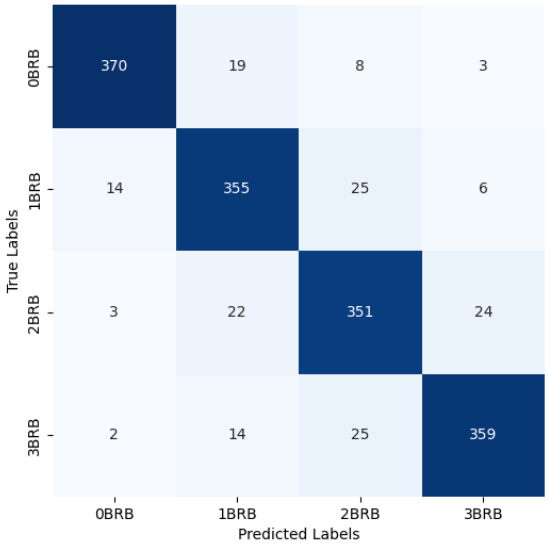

Figure 4.13: Confusion Matrix for Combined Load Level

Table 4.5: Performance of the MLP at various load levels

Parameters	**25% of Rated Load**	**50% of Rated Load**	**75% of Rated Load**	**100% of Rated Load**	**Combined Load Levels**
Accuracy (%)	82.5	87.25	92.75	96.25	89.69
Precision (%)	89.47	95.74	96.96	98.01	95.11
Recall (%)	85	90	96	99	92.5
F1-score (%)	87.17	92.78	96.47	98.50	93.78

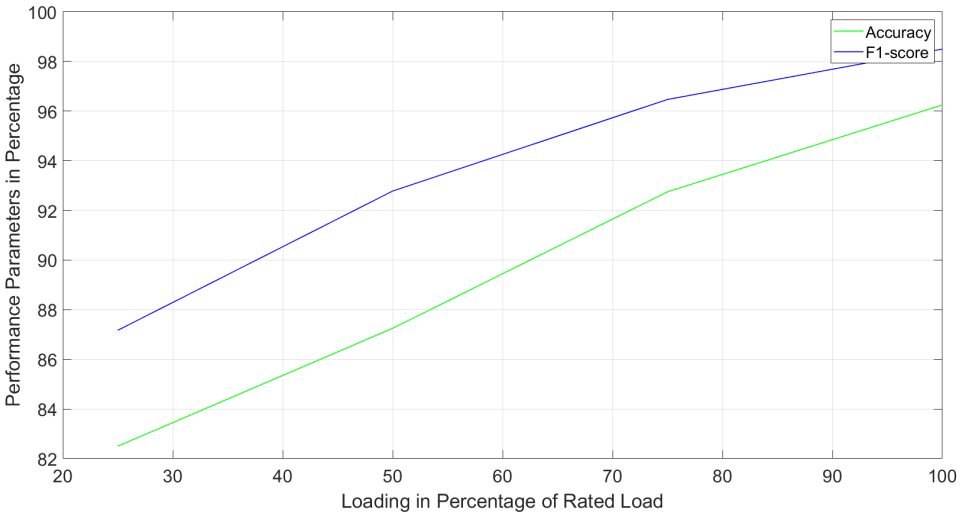

Figure 4.14: Performance of the MLP at various load levels

From Table 4.5 and Figure 4.14, the following observations could be made:

Increased Performance with Load: The accuracy and f1-score of the monitoring technique consistently increases with higher machine loads. This trend suggests that the presented technique is more effective at detecting and classifying faults as the machine operates closer to its maximum capacity.

Incremental Improvement: There is a noticeable incremental improvement in performance of the presented technique as the load progresses from 25% to full load. This progressive increase in the performance indicates that the method becomes more reliable and sensitive to detecting fault-related signals as the loading conditions become more demanding.

High Accuracy at Full Load: Achieving a high accuracy of 96.25% at full load indicates that the monitoring technique performs exceptionally well under optimal operating conditions. This high level of accuracy is crucial for reliable fault detection and predictive maintenance in industrial settings.

Therefore, it can be concluded that the performance of the monitoring technique correlates positively with increasing machine load. This conclusion underscores the technique's capability to effectively monitor and diagnose machine health across different operational conditions, with higher accuracy observed at higher load levels.

CHAPTER FIVE: CONCLUSION

In this research, frequency analysis was presented as a way to detect the broken rotor faults in induction machine. It is also shown that by observing the side bands around the fundamental frequency, the broken rotor faults in induction machine could be detected. Furthermore, an MLP model was trained to detect the faults from the measured features. Further, investigation is needed to detect the fault during the lower loading of the machine.

The effectiveness of the presented condition monitoring technique noticeably improved as the percentage loading of the machine increased. This enhancement in performance at higher load levels can be primarily attributed to the amplified magnitude of the sidebands in the current signal. Side bands, which represent frequencies related to broken bar faults, become more pronounced as the load on the machine increases. Moreover, the increase in machine load results in these sidebands shifting further away from the fundamental component of the signal. This separation makes it easier for the monitoring technique to distinguish between different states or conditions of the machine based on the frequency components present in the current signal. On the other hand, the relative lower performance of the monitoring technique at low loading levels is primarily due to the diminished amplitude and proximity of side bands to the fundamental component in the current signal. These factors reduce the clarity and separability of fault-related frequencies.

Therefore, the condition monitoring technique benefits significantly from higher load levels due to both the increased amplitude and clearer differentiation of side bands. This correlation underscores the technique's sensitivity to detecting and identifying faults under varying operational conditions, thereby enhancing the reliability and effectiveness of machine health assessments in practical applications.

REFERENCES

[1] N. Sarma, P. Tuohy, and S. Djurovic, "Condition monitoring of rotating electrical machines," in *Encyclopedia of Electrical and Electronic Power Engineering*, 2023, pp. 143–154.

[2] T. Vaimann and A. Kallaste, "Condition monitoring of electrical machines," *11th Int. Symp."Topical problems in the field of el. and power eng*, pp. 209–212, 01 2012.

[3] J. Rangel-Magdaleno, J. Ramirez-Cortes, and H. Peregrina-Barreto, "Broken bars detection on induction motor using mcsa and mathematical morphology: An experimental study," in *2013 IEEE International Instrumentation and Measurement Technology Conference (I2MTC)*, 2013, pp. 825–829.

[4] F. Mansour, "Induction motors: Construction, principle of operation, power and torque calculations, characteristics and speed control," 06 2020.

[5] P. F. Albrecht, J. C. Appiarius, R. M. McCoy, E. L. Owen, and D. K. Sharma, "Assessment of the reliability of motors in utility applications - updated," *IEEE Power Engineering Review*, vol. PER-6, no. 3, pp. 31–32, 1986.

[6] O. Thorsen and M. Dalva, "A survey of faults on induction motors in offshore oil industry, petrochemical industry, gas terminals, and oil refineries," *IEEE Transactions on Industry Applications*, vol. 31, no. 5, pp. 1186–1196, 1995.

[7] "Report of large motor reliability survey of industrial and commercial installations, part i," *IEEE Transactions on Industry Applications*, vol. IA-21, no. 4, pp. 853–864, 1985.

[8] "Report of large motor reliability survey of industrial and commercial installations, part ii," *IEEE Transactions on Industry Applications*, vol. IA-21, no. 4, pp. 865–872, 1985.

[9] S. Bindu and V. V. Thomas, "Diagnoses of internal faults of three phase squirrel cage induction motor — a review," in *2014 International Conference on Advances in Energy Conversion Technologies (ICAECT)*, 2014, pp. 48–54.

[10] S. Nandi, R. Bharadwaj, H. Toliyat, and A. Parlos, "Study of three phase induction motors with incipient rotor cage faults under different supply conditions," in *Conference Record of the 1999 IEEE Industry Applications Conference. Thirty-Forth IAS Annual Meeting (Cat. No.99CH36370)*, vol. 3, 1999, pp. 1922–1928 vol.3.

[11] A. Guedidi, W. Laala, A. Guettaf, and S. E. Zouzou, "Diagnosis and classification of broken bars fault using dwt and artificial neural network without slip estimation," in *2020 XI International Conference on Electrical Power Drive Systems (ICEPDS)*, 2020, pp. 1–7.

[12] I. Ouachtouk, S. El Hani, S. Guedira, K. Dahi, and H. Mediouni, "Broken rotor bar fault detection based on stator current envelopes analysis in squirrel cage induction machine," in *2017 IEEE International Electric Machines and Drives Conference (IEMDC)*, 2017, pp. 1–6.

[13] Y. Xie, Z. Wang, X. Shan, and Y. Li, "Investigation of rotor thermal stress in squirrel cage induction motor with broken bar faults," *COMPEL - The international journal for computation and mathematics in electrical and electronic engineering*, 2015.

[14] M. R. Hans and P. D. Mane, "Detection of broken rotor bar along with thermal overload protection," in *2017 2nd International Conference on Communication and Electronics Systems (ICCES)*, 2017, pp. 414–419.

[15] P. Tanver, L. Ran, J. Penman, and H. Seeding, *Condition Monitoring of Rotating Electrical Machines*. Stevenage, UK: The Institution of Engineering and Technology, 2008.

[16] B. Amel, Y. Laatra, S. Sami, and D. Nourreddine, "Classification and diagnosis of broken rotor bar faults in induction motor using spectral analysis and svm," in *2013 Eighth International Conference and Exhibition on Ecological Vehicles and Renewable Energies (EVER)*, 2013, pp. 1–5.

[17] A. Belahcen, J. Martinez, and T. Vaimann, "Comprehensive computations of the response of faulty cage induction machines," in *2014 International Conference on Electrical Machines (ICEM)*, 2014, pp. 1510–1515.

APPENDIX A: PUBLICATION

Conference paper

[IOEGC15] Editor Decision

2024-06-09 08:40 AM

Chandan Pokhrel; Nava Raj Karki, Basanta Kumar Gautam:

We have reached a decision regarding your submission to 15th IOE Graduate Conference, "Analysis of Effects of Loading Conditions on Condition Monitoring of Induction Machines".

Our decision is to: **Accept Submission**

[*This email is auto-generated from 15th IOE Graduate Conference web portal*]

Analysis of Effects of Loading Conditions on Condition Monitoring of Induction Machines

Chandan Pokhrel [a], Nava Raj Karki [b], Basanta Kumar Gautam [c]

[a] *Department of Electrical Engineering, Pulchowk Campus, Institute of Engineering, Tribhuvan University, Nepal*
[b] *Department of Electrical Engineering, Pulchowk Campus, Institute of Engineering, Tribhuvan University, Nepal*
[c] *Department of Electrical Engineering, Pulchowk Campus, Institute of Engineering, Tribhuvan University, Nepal*
[a] 078mspse006.chandan@pcampus.edu.np

Abstract
Induction machines are used in a different range of applications because of their low cost, robustness, and high efficiency. All machines, no matter how robust they are or how well they are designed, are prone to faults during their operation. Broken rotor bar faults is one of such faults and can cause a number of unwanted effects in induction motors. Condition monitoring is required to detect those faults in its inception stage to minimize the down time, economic losses and safety risks. The broken rotor fault produces the sidebands components around the fundamental frequency. By analysing the frequency spectrum of the motor input current for the sidebands, the broken rotor fault can be detected. In this paper, Discrete Fourier Transform is used to analyze the input current of the squirrel cage induction motor to study the effects of the variation of the changing load level on the sidebands to differentiate between healthy and faulty motor states.

Keywords
Induction Motor, Condition Monitoring, Fourier Transform, Broken Rotor Bars

1. Introduction

1.1 Background

Electrical machines are used in a vast number of applications, including but not limited to those in home appliances, electric vehicles, manufacturing process, and power generation. These electrical machines come in various sizes, ranging from a fraction of kilowatts used in household applications, to hundreds of megawatts used in electricity generation. Among them the induction machine consumes around 85% of power in the industrial applications[1]. Induction machine finds its various applications because of its low cost, high efficiency, and robustness[2]. But, no matter how robust a machine is, it is prone to failure at some point of its lifetime. Some of the induction machine faults are broken rotor faults, eccentricity faults, bearing faults, single phasing, and stator winding short circuits. Although broken rotor bars represent around 10% of motor failure, depending on the failure level, they may produce total motor loss[1]. Condition monitoring is the detection of the faults in its inception states before leading to catastrophic failure in order to minimize the down time, economic losses, safety risks, and total motor loss.

1.2 Causes of broken rotor bar

Broken rotor bar faults occur when one or more of the bars that make up the rotor breaks. The failure is caused by the combination of one or more of the following[3, 4].

- Overheating of the rotor cage due to direct on-line starting or overloading.
- Mechanical stress due to pulsating loads, unbalanced load, bearing failures, excessive vibrations, and voltage fluctuations.
- Magnetic stress due to unbalanced electromagnetic forces.
- Contamination and corrosion due to chemical or moisture exposure.
- Manufacturing defects.

1.3 Effects of broken rotor bar on machine operation

A broken rotor bar carries little to no current depending on the degree of the fault. This causes rotor current to be unbalanced[5]. A motor can operate in this asymmetrical condition but results in unbalanced air gap flux, increased losses, increased torque oscillations and decrease in average torque[6]. Due to increase in losses and decrease in average torque, the motor slip increases at constant load as the severity of the fault increases. As the broken bar is unable to conduct the current originally flowing through it, the currents in the neighboring bar increases. Figure 1 [7] shows the current density distribution of squirrel cage motor under healthy and faulty conditions. It shows that the current density increases in the bar close to the broken bar and the effect is more pronounced as the severity of the fault increases. This increase in current leads to an increase in temperature of the rotor and increase losses since the heat loss is directly proportional to the square of the current flowing through it. This increase in heat and temperature of the rotor bar causes the rotor to expand and thus increases the tension in the bar. Increased temperature, electrical stress, and mechanical stress will deform the rotor over time and increase the failure probability of the adjacent rotor bar. This can then escalate to other rotor bars.

In the motor with the high rotor speed, the broken rotor bar may experience sufficient centrifugal forces and can bend toward the stator. This rotor bar may then come in contact with the stator winding leading to the motor failure[8].

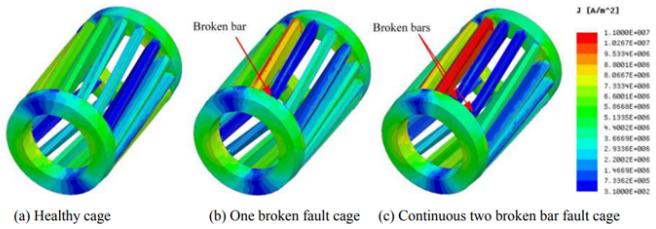

Figure 1: The current density distribution of squirrel cage machine at healthy and faulty condition[7]

2. Methodology

This section describes the experimental method, and the tools and technique used to detect the broken rotor bar faults in the induction machine. The method used here is an non-invasive condition monitoring technique and does not require the direct access to the motor for its implementation. This method requires the stator current of the motor which is easily accessible since, it is utilized for the protection of motor from over currents.

2.1 Stator Current Sidebands

The stator input current contains the information about the machine health. The operation of the induction machine with broken rotor bar induces the line currents at the frequencies given by[9, 10]

$$\mathbf{f_{brb}} = \mathbf{f_s}(\mathbf{m} \pm \mathbf{2ks})$$

where,
$\mathbf{m}$ = 1, 3, 5, ...
$k \in \mathbb{N}^+$
$\mathbf{f_s}$ is the fundamental component of the stator current
$\mathbf{s}$ is the motor slip

which are known as the side band components. An increment in the magnitude of theses characteristics frequency in the stator current indicates a rotor bar fault. Therefore, the study of these frequencies is a viable option to differentiate motor states.

The magnitude of the components in $\mathbf{f_{brb}}$ decreases rapidly with increase in $\mathbf{k}$ and $\mathbf{m}$. This is shown in Figure 2[11] and as such they are often limited to 3. In this paper, the sidebands

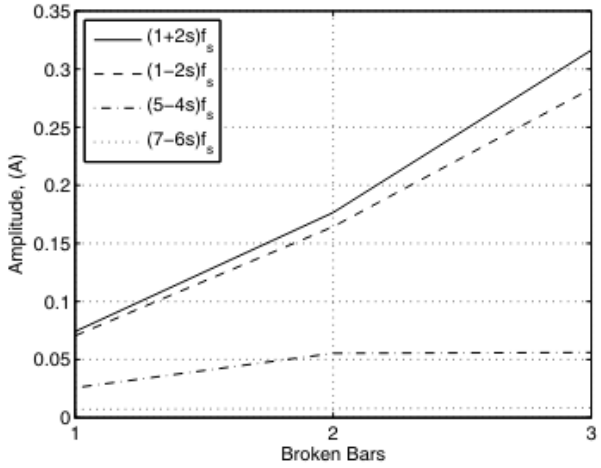

Figure 2: Variation of the magnitue of sidebands

corresponding to $\mathbf{k} = 1$ and $\mathbf{m} = 1$ is studied. The sideband $\mathbf{f_s}(\mathbf{1} - \mathbf{2s})$ is termed as Left Side Band (LSB) and $\mathbf{f_s}(\mathbf{1} + \mathbf{2s})$ is termed as Right Side Band (RSB).

2.2 Experimental Setup

The stator input currents for both healthy and faulty states was obtained from the experimental setup at Aalto University, Finland and Tallin University of Technology, Estonia.The machine specification is shown in Table 1.

Parameters	Units	Value
Number of poles		4
Number of Phases		3
Connection		Δ
Voltage	V	400
Current	A	15.3
Power	kW	7.5
Speed	rpm	1460
Power factor		0.79

Table 1: Machine Parameters

The experimental setup is shown in Figure 3. The experiment consists of two identical motors connected back-to-back through their shaft and placed on the same mechanical base. The first healthy motor is use to load the second motor which had 0 to 3 Broken rotor bars. Broken rotor bars were implemented by drilling a hole through the rotor.

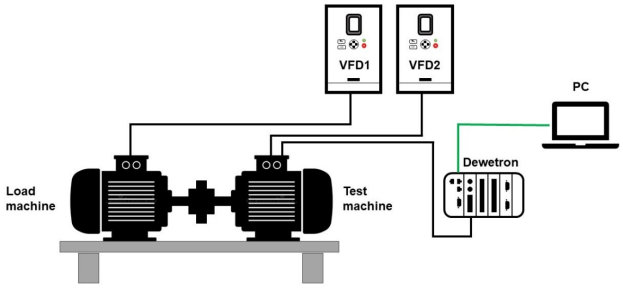

Figure 3: Block diagram of the setup

First, the test machine's phase current was recorded for 20 seconds after steady state under healthy conditions (i.e., at 0 broken rotor bar fault) at different load levels of 0, 25, 50, 75, and 100 percent of the rated nominal load at the sampling rate of 20kHz. Next the rotor bar was broken by drilling a hole in the rotor slot. The bars were broken sequentially, and the current signal recordings were obtained for 1, 2, and 3 broken rotor state. The recordings were stored in a .mat files. Figure 4 - Figure 6 shows the sample measured current signal of the test machine at different states. From, Figure 4 - Figure 6, it can be seen that the machine states are difficult to differentiate based only on time domain signal. Hence, the Discrete Fourier Transform (DFT) was applied to the measured current signals to obtain the frequency spectrum.

2.3 Discrete Fourier Transform

Let x_n be a sequence of the N measured values.

$$x_n = x_0, x_1, x_2, ..., x_{N-1}$$

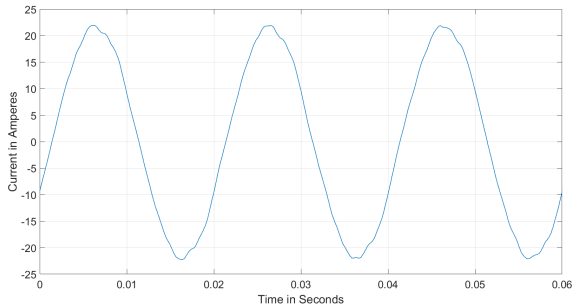

Figure 4: Current Profile from Test Machine with 0 Broken Rotor Bar at 100% Load

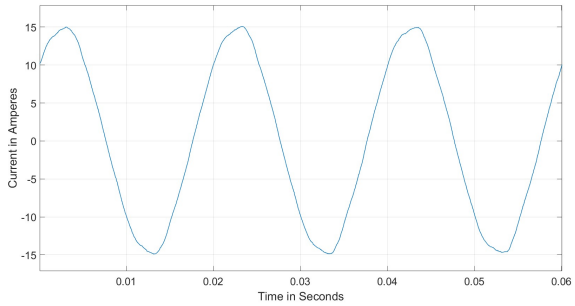

Figure 5: Current Profile from Test Machine with 3 Broken Rotor Bar at 50% Load

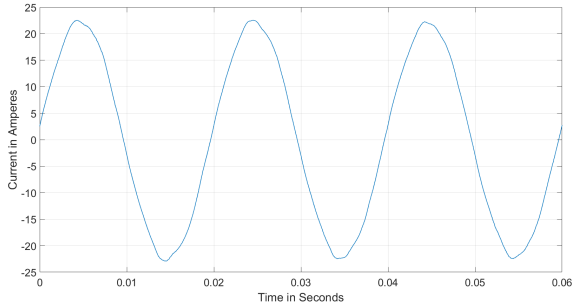

Figure 6: Current Profile from Test Machine with 3 Broken Rotor Bar at 100% Load

Then the DFT of the sequence x_n is defined as

$$X_K = \frac{1}{N}\sum_{n=0}^{N-1} e^{-\frac{j2\pi Kn}{N}}$$

where $X_K = X_0, X_1, ..., X_{N-1}$ is the DFT of the sequence x_n and j is the imaginary unit.

3. Result and Discussion

Figure 7 - 11 shows the DFT of the measured current signal at various load levels and various healthy and faulty states. The states are labeled as below:

- Healthy: Motor with no broken rotor bar faults
- 1BRB: Motor with one broken rotor bar
- 2BRB: Motor with two consecutive broken rotor bars

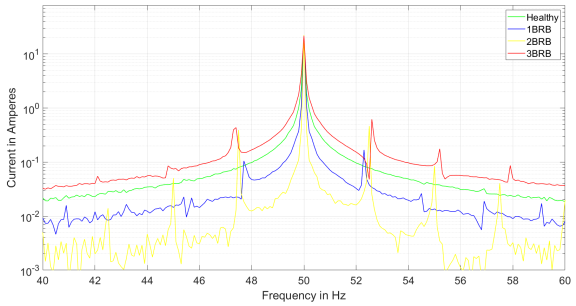

Figure 7: Frequency Spectra of Motors with Healthy and Broken Rotor Bars at 100% of rated load

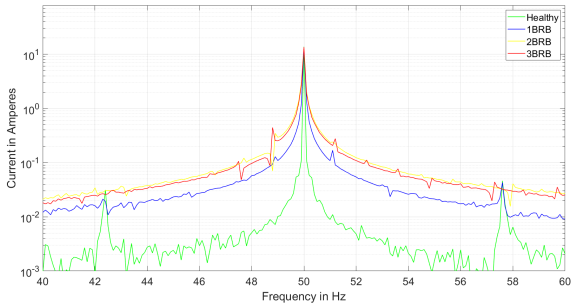

Figure 8: Frequency Spectra of Motors with Healthy and Broken Rotor Bars at 75% of rated load

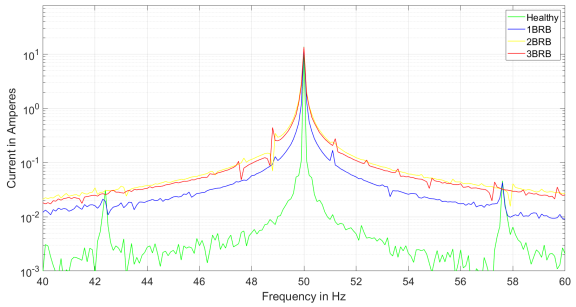

Figure 9: Frequency Spectra of Motors with Healthy and Broken Rotor Bars at 50% of rated load

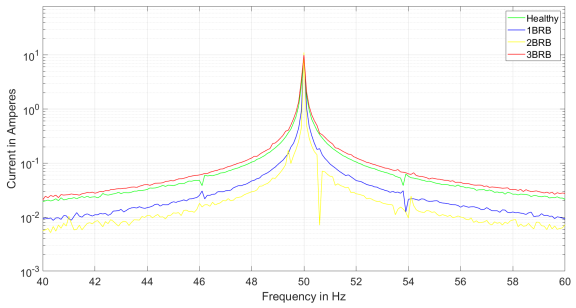

Figure 10: Frequency Spectra of Motors with Healthy and Broken Rotor Bars at 25% of rated load

- 3BRB: Motor with three consecutive broken rotor bars.

From the frequency spectra shown in Figure 7-11, it can be easily seen that the side band arises around the fundamental component. The magnitude of the bands at either side of the fundamental frequency was found to increase with the increase in the severity

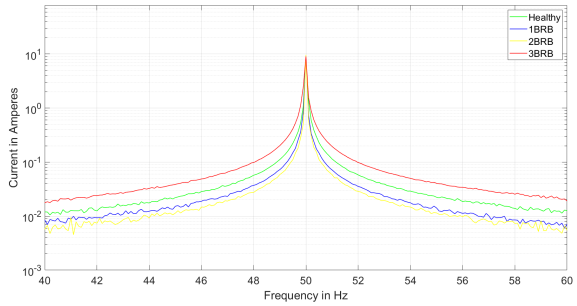

Figure 11: Frequency Spectra of Motors with Healthy and Broken Rotor Bars at 0% of rated load

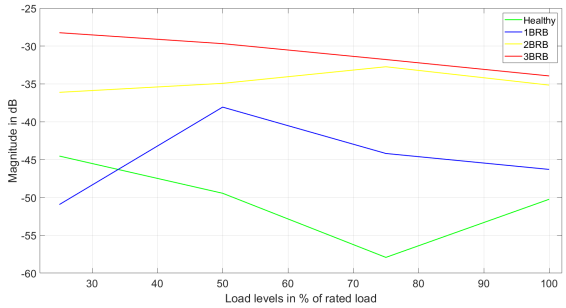

Figure 12: Magnitude of Left Side Band at various load levels

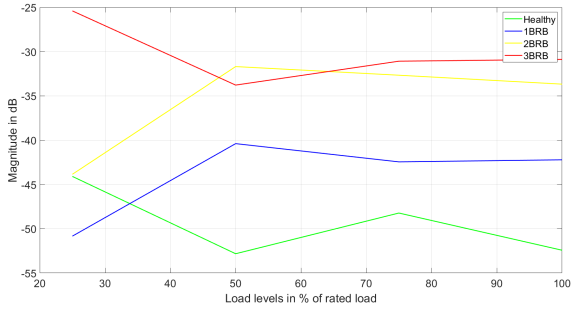

Figure 13: Magnitude of Right Side Band at various load levels

of the fault. Also, the side bands were found to shift away from the fundamental component with the increase in severity of the fault. The sidebands were difficult to observe in low and no load condition on both healthy and faulty states. Further Figure 12 and Figure 13 shows the variation of the magnitude of the side bands around the fundamental frequency which can be used to detect the broken rotor bar faults in induction machine. The reason for the difficulty to detect the sidebands at low and no load conditions is due to the fact that the slip $\mathbf{s}$ decreases with the decrease in loading of the motor and the side band frequencies given by $\mathbf{f_s(1-2s)}$ and $\mathbf{f_s(1+2s)}$ shifts close to the supply frequency $\mathbf{f_s}$. Also, the decrease in the magnitude of the input current at lower loading causes the sidebands to decrease in magnitudes, further making it difficult for their detection.

4. Conclusion

In this paper, frequency analysis was presented as a way to detect the broken rotor faults in induction motor. Section 3 showed that by observing the side bands around the fundamental frequency, the broken rotor faults in induction motor could be detected. An ANN model could be trained to detect the faults in the motors efficiently. Further investigation is needed to detect the fault during the lower loading of the machine.

Acknowledgments

This work was supported by the Department of Electrical Engineering and Automation, Aalto University, Finland under the project Capacity Enhancement of Electrical Equipment Condition Monitoring and Fault Diagnostics (CEEECoM).

References

[1] J. Rangel-Magdaleno, J. Ramirez-Cortes, and H. Peregrina-Barreto, "Broken bars detection on induction motor using mcsa and mathematical morphology: An experimental study," in *2013 IEEE International Instrumentation and Measurement Technology Conference (I2MTC)*, pp. 825–829, 2013.

[2] C. Terron-Santiago, J. Martinez-Roman, R. Puche-Panadero, and A. Sapena-Bano, "A review of techniques used for induction machine fault modelling," *Sensors (Basel, Switzerland)*, 2021.

[3] S. Bindu and V. V. Thomas, "Diagnoses of internal faults of three phase squirrel cage induction motor — a review," in *2014 International Conference on Advances in Energy Conversion Technologies (ICAECT)*, pp. 48–54, 2014.

[4] S. Nandi, R. Bharadwaj, H. Toliyat, and A. Parlos, "Study of three phase induction motors with incipient rotor cage faults under different supply conditions," in *Conference Record of the 1999 IEEE Industry Applications Conference. Thirty-Forth IAS Annual Meeting (Cat. No.99CH36370)*, vol. 3, pp. 1922–1928 vol.3, 1999.

[5] A. Guedidi, W. Laala, A. Guettaf, and S. E. Zouzou, "Diagnosis and classification of broken bars fault using dwt and artificial neural network without slip estimation," in *2020 XI International Conference on Electrical Power Drive Systems (ICEPDS)*, pp. 1–7, 2020.

[6] I. Ouachtouk, S. El Hani, S. Guedira, K. Dahi, and H. Mediouni, "Broken rotor bar fault detection based on stator current envelopes analysis in squirrel cage induction machine," in *2017 IEEE International Electric Machines and Drives Conference (IEMDC)*, pp. 1–6, 2017.

[7] Y. Xie, Z. Wang, X. Shan, and Y. Li, "Investigation of rotor thermal stress in squirrel cage induction motor with broken bar faults," *COMPEL - The international journal for computation and mathematics in electrical and electronic engineering*, 2015.

[8] M. R. Hans and P. D. Mane, "Detection of broken rotor bar along with thermal overload protection," in *2017 2nd International Conference on Communication and Electronics Systems (ICCES)*, pp. 414–419, 2017.

[9] I. Ouachtouk, S. El Hani, S. Guedira, and K. Dahi, "Detection and classification of broken rotor bars faults in induction machine using k-means classifier," in *2016 International Conference on Electrical and Information Technologies (ICEIT)*, pp. 180–185, 2016.

[10] B. Amel, Y. Laatra, S. Sami, and D. Nourreddine, "Classification and diagnosis of broken rotor bar faults in induction motor using spectral analysis and svm," in *2013 Eighth International Conference and Exhibition on Ecological Vehicles and Renewable Energies (EVER)*, pp. 1–5, 2013.

[11] G. R. Bossio, C. H. De Angelo, C. M. Pezzani, J. M. Bossio, and G. O. Garcia, "Evaluation of harmonic current sidebands for broken bar diagnosis in induction motors," in *2009 IEEE International Symposium on Diagnostics for Electric Machines, Power Electronics and Drives*, pp. 1–6, 2009.

APPENDIX B: PLAGIARISM TEST REPORT

Analysis of Effects of Loading Conditions on Condition Monitoring of Induction Machines

ORIGINALITY REPORT

13%
SIMILARITY INDEX

PRIMARY SOURCES

1	www.mdpi.com Internet	85 words — 1%
2	www.ijraset.com Internet	56 words — 1%
3	hdl.handle.net Internet	38 words — < 1%
4	Bhukya Ramadevi, Venkata Ramana Kasi, Kishore Bingi. "Fractional ordering of activation functions for neural networks: A case study on Texas wind turbine", Engineering Applications of Artificial Intelligence, 2024 Crossref	35 words — < 1%
5	www.coursehero.com Internet	35 words — < 1%
6	uia.brage.unit.no Internet	33 words — < 1%
7	Huiliang Cao, Yingjie Zhang, Ziqi Han, Xingling Shao, Jinyang Gao, Kun Huang, Yunbo Shi, Jun Tang, Chong Shen, Jun Liu. "Pole-Zero-Temperature Compensation Circuit Design and Experiment for Dual-mass MEMS Gyroscope Bandwidth Expansion", IEEE/ASME Transactions on Mechatronics, 2019	32 words — < 1%

Crossref

8	Makhetha, Mamakhetha Eveline. "Effect of Rotor Bar Shape and Stator Slot Opening on a Three Phase Induction Motor with Broken Bars", University of Johannesburg (South africa), 2021 ProQuest	29 words — < 1%
9	ir.jkuat.ac.ke Internet	28 words — < 1%
10	etda.libraries.psu.edu Internet	27 words — < 1%
11	www.medrxiv.org Internet	23 words — < 1%
12	Abiodun Ayodeji, Yong-kuo Liu. "SVR optimization with soft computing algorithms for incipient SGTR diagnosis", Annals of Nuclear Energy, 2018 Crossref	22 words — < 1%
13	Malaya Kumar Hota. "Identification of protein-coding regions in eukaryotes using Fourier Transforms and Singular Value Decomposition using multiple length sliding windows", International Journal of Signal and Imaging Systems Engineering, 2011 Crossref	21 words — < 1%
14	arxiv.org Internet	19 words — < 1%
15	doczz.net Internet	18 words — < 1%
16	Gaeid, Khalaf Salloum. "Wavelet Based Fault Tolerant Control of Induction Motor", University	16 words — < 1%

of Malaya (Malaysia), 2023
ProQuest

17	aclanthology.org Internet	16 words — < 1%
18	www.diva-portal.org Internet	16 words — < 1%
19	digitalcommons.latech.edu Internet	15 words — < 1%
20	link.springer.com Internet	15 words — < 1%
21	www.ir.nctu.edu.tw Internet	15 words — < 1%
22	lutpub.lut.fi Internet	14 words — < 1%
23	5dok.org Internet	13 words — < 1%
24	Ivan Stoychev, Philipp Wehner, Jens Rettkowski, Tobias Kalb, Patrick Wichert, Diana Göhringer, Jürgen Oehm. "Sensor data fusion in the context of electric vehicles charging stations using a Network-on-Chip", Microprocessors and Microsystems, 2018 Crossref	13 words — < 1%
25	datasciencenerd.com Internet	13 words — < 1%
26	lcbda.punjab.gov.pk Internet	13 words — < 1%

27	umpir.ump.edu.my Internet	13 words — < 1%
28	de Carvalho Pereira Ferreira, Inês. "Churn Prediction in Digital Marketing", Universidade do Porto (Portugal), 2024 ProQuest	12 words — < 1%
29	theses.ncl.ac.uk Internet	12 words — < 1%
30	Khodsuz, Masume, and Mohammad Mirzaie. "An improved time-delay addition method for MOSA resistive leakage current extraction under applied harmonic voltage", Measurement, 2016. Crossref	11 words — < 1%
31	Samia Bourdim, Kamel Eddine Hemsas, Youcef Harbouche. "Intelligent Diagnostic of Induction Machine for Faults Detection and Classification Using Wavelet and Fuzzy Inference", Applied Mechanics and Materials, 2015 Crossref	11 words — < 1%
32	cdn.slideserve.com Internet	11 words — < 1%
33	B. Asad, T. Vaimann, A. Belahcen, A. Kallaste, A. Rassolkin, H. Heidari. "The Low Voltage Start-up Test of Induction Motor for the Detection of Broken Bars", 2020 International Conference on Electrical Machines (ICEM), 2020 Crossref	10 words — < 1%
34	Kishorebabu Dasari. "Evaluation of UDP-Based DDoS Attack Detection by Neural Network Classifier with Convex Optimization and Activation Functions", Ingénierie des systèmes d information, 2024 Crossref	10 words — < 1%

35	aranne5.bgu.ac.il Internet	10 words — < 1%
36	bmcmedinformdecismak.biomedcentral.com Internet	10 words — < 1%
37	Clobes, M.. "Shape-dependent characteristics of full-scale wind profiles", Journal of Wind Engineering & Industrial Aerodynamics, 201109 Crossref	9 words — < 1%
38	d197for5662m48.cloudfront.net Internet	9 words — < 1%
39	elibrary.tucl.edu.np Internet	9 words — < 1%
40	nagoya.repo.nii.ac.jp Internet	9 words — < 1%
41	repository.mines.edu Internet	9 words — < 1%
42	smartech.gatech.edu Internet	9 words — < 1%
43	uis.brage.unit.no Internet	9 words — < 1%
44	"Advances in Data and Information Sciences", Springer Science and Business Media LLC, 2024 Crossref	8 words — < 1%
45	"Proceedings of Emerging Trends and Technologies on Intelligent Systems", Springer Science and Business Media LLC, 2023 Crossref	8 words — < 1%

46 A.G. Parlos. "Study of three phase induction motors with incipient rotor cage faults under different supply conditions", Conference Record of the 1999 IEEE Industry Applications Conference Thirty-Forth IAS Annual Meeting (Cat No 99CH36370) IAS-99, 1999
Crossref
8 words — < 1%

47 Arévalo, Emilio Perfecto Martínez. "Classification of Public Procurement Procedures Based on Red Flags with a Machine Learning Approach for the Detection of Possible Risk of Corruption", Centro de Investigacion y Docencia Economicas (Mexico), 2024
ProQuest
8 words — < 1%

48 Jing Sun. "A Method of Realizing the Reliable Operation of the Variable Frequency Drive – Hot Backup Switching", Journal of Physics: Conference Series, 2022
Crossref
8 words — < 1%

49 Mangwiro, Vhalani Virginia. "Strategic Planning and Risk Analysis to Prevent Induction Motor Failure", University of Johannesburg (South Africa), 2021
ProQuest
8 words — < 1%

50 Parikh, Prayag Kiritkumar. "Use of Bus-Level Electrical Signals for Improving Power Plant Operations.", The University of North Carolina at Charlotte, 2020
ProQuest
8 words — < 1%

51 Patel, Jaykumar. "Classifying Galaxy Images Using Improved Residual Networks", University of Windsor (Canada), 2023
ProQuest
8 words — < 1%

52 R. Bharadwaj. "Detection of induction motor faults-combining signal-based and model-based
8 words — < 1%

techniques", Proceedings of the 2002 American Control Conference (IEEE Cat No CH37301) ACC-02, 2002
Crossref

53 Sasi, A.Y.B.. "A validated model for the prediction of rotor bar failure in squirrel-cage motors using instantaneous angular speed", Mechanical Systems and Signal Processing, 200610
Crossref
8 words — < 1%

54 Xie, Zhongliang. "Earthquake Induced Inelastic Demands on Buckling Restrained Braces", Auburn University, 2023
ProQuest
8 words — < 1%

55 ar5iv.labs.arxiv.org
Internet
8 words — < 1%

56 arts.units.it
Internet
8 words — < 1%

57 digi.lib.ttu.ee
Internet
8 words — < 1%

58 dspace.atilim.edu.tr
Internet
8 words — < 1%

59 ethesis.nitrkl.ac.in
Internet
8 words — < 1%

60 ntnuopen.ntnu.no
Internet
8 words — < 1%

61 prr.hec.gov.pk
Internet
8 words — < 1%

62 wrap.warwick.ac.uk
Internet
8 words — < 1%

63	www.techscience.com Internet	8 words — < 1%
64	Ebrahimi, B.M.. "Novel indices for broken rotor bars fault diagnosis in induction motors using wavelet transform", Mechanical Systems and Signal Processing, 201207 Crossref	7 words — < 1%
65	K. V. Arunima, Kartikeya Bolar. "chapter 1 Integrating Diversity, Equity, and Inclusion (DEI) Effectiveness Metrics Into Recruitment Analytics", IGI Global, 2023 Crossref	7 words — < 1%
66	A.R. Sadeghian. "Signature analysis of induction motor mechanical faults by wavelet packet decomposition", APEC 2001 Sixteenth Annual IEEE Applied Power Electronics Conference and Exposition (Cat No 01CH37181) APEC-01, 2001 Crossref	6 words — < 1%
67	Aryanfar, Asghar. "Dendrites Inhibition in Rechargeable Lithium Metal Batteries.", Proquest, 2015. ProQuest	6 words — < 1%
68	Jiang, Saibiao. "Fault Diagnosis of Induction Motors Under Untrained Loads with a Feature Adaptation and Improved Broad Learning Framework", University of Macau, 2023 ProQuest	6 words — < 1%

EXCLUDE QUOTES ON EXCLUDE SOURCES OFF